Journal of Earthquake Engineering
Publication details, including instructions for authors and subscription information:
http://www.tandfonline.com/loi/ueqe20

Shaking Table Testing of Rocking—Isolated Bridge Pier on Sand

I. Anastasopoulos [a], M. Loli [a], T. Georgarakos [a] & V. Drosos [a]
[a] School of Civil Engineering, National Technical University of Athens, Athens, Greece

Version of record first published: 18 Dec 2012.

To cite this article: I. Anastasopoulos , M. Loli , T. Georgarakos & V. Drosos (2013): Shaking Table Testing of Rocking—Isolated Bridge Pier on Sand, Journal of Earthquake Engineering, 17:1, 1-32

To link to this article: http://dx.doi.org/10.1080/13632469.2012.705225

Journal of Earthquake Engineering, 17:1–32, 2013

ISSN: 1363-2469 print / 1559-808X online
DOI: 10.1080/13632469.2012.705225

Taylor & Francis
Taylor & Francis Group

Shaking Table Testing of Rocking–Isolated Bridge Pier on Sand

I. ANASTASOPOULOS, M. LOLI, T. GEORGARAKOS, and V. DROSOS

School of Civil Engineering, National Technical University of Athens, Athens, Greece

This article studies the seismic performance of a rocking-isolated *bridge pier on surface foundation, resting on sand. A series of reduced-scale shaking table tests are conducted, comparing the performance of a rocking-isolated system to a pier founded on* conventionally designed foundation. *The two design alternatives are subjected to a variety of shaking events, comprising real records and artificial motions of varying intensity. In an effort to explore system performance in successive seismic events, three different shaking sequences are performed.* Rocking isolation *is proven quite effective in reducing the inertia forces transmitted onto the superstructure. The rocking-isolated pier is effectively protected, surviving all seismic excitations without structural damage, at the cost of increased foundation settlement. In contrast, a certain degree of structural damage would be unavoidable for the same system founded on a conventionally designed foundation. The rocking-isolated system is proven remarkably resistant to cumulative cyclic loading, exhibiting limited strength degradation even when subjected to cyclic drift ratio in excess of 5.5%. Due to soil densification, the rate of settlement accumulation is found to decrease with repeating seismic excitations. The rotational response is practically insensitive to the shaking history when the preceding seismic motions are* symmetric *(such as sinusoidal motions). In stark contrast, when the preceding seismic motions are* non-symmetric *(such as the directivity-affected records of this study), the system tends to accumulate rotation after each event, progressively worsening its performance. Nevertheless, the rocking-isolated system survives toppling collapse, even when subjected to a highly improbable, unrealistically harsh, sequence of seismic events.*

Keywords Rocking; Shaking Table; Seismic Isolation; Soil Nonlinearity; Ductility; Strength Degradation

1. Introduction

The concept of *"rocking isolation"* [Mergos and Kawashima, 2005] can be traced back in the early work of Housner [1963] and Meek [1975], where the potentially beneficial role of foundation rocking was first pointed out. Allowed to rock, the foundation sets a limit on the inertia loading that may be transmitted onto the superstructure, acting as a means of seismic isolation. The potential benefits of such seismic design concept have been verified by several studies (e.g., Beck and Skinner, 1974; Huckelbridge and Ferencz, 1981; Priestley *et al.*, 1996; Chen *et al.*, 2006; Sakellaraki and Kawashima, 2006; Palmeri and Makris, 2008; Algie *et al.,* 2009; Hung *et al.*, 2011), and reservedly employed in practice mostly for the retrofit of existing structures [ATC-40; FEMA, 1997; Dowdell and Harmersley,

Received 20 August 2011; accepted 14 June 2012.
Address correspondence to I. Anastasopoulos, School of Civil Engineering, National Technical University of Athens, Athens, Greece. E-mail: ianast@civil.ntua.gr

2000], but also in a few cases of newly designed large-size ("monumental") bridges (e.g., Yashinsky and Karshenas, 2003; Pecker, 2005).

However, modern seismic codes (e.g., EC8) tend to prohibit the application of such concepts by not allowing mobilization of foundation capacity, aiming to guide the "plastic hinge" to the superstructure, the behavior of which is believed to be more controllable, not being affected by uncertainties related to soil properties. The most important reason behind this conservatism is the inherent "fear" that mobilization of foundation capacity, either in the form of uplifting or soil yielding underneath the foundation, may lead to toppling collapse of the structure. Yet, thanks to the *kinematic* and *cyclic* nature of seismic loading, mobilization of the above mechanisms is very far from leading to collapse: only limited rotation and settlement may take place before reversal of the direction of loading. Naturally, the toppling potential of a seismic motion will be a function of its dominant frequency, as demonstrated in various studies related to rigid blocks rocking on rigid base (e.g., Zhang and Makris, 2001; Apostolou *et al.*, 2007).

Aiming at alleviating the above skepticism, extensive research has been conducted to gain insights and quantify the main aspects of strongly nonlinear foundation response. A variety of analytical studies is readily available in the literature, ranging from finite element (FE) or finite differences numerical analysis of the entire soil–foundation–structure system (e.g., Taiebat and Carter, 2000; Gourvenec 2007; Anastasopoulos *et al.*, 2011; Panagiotidou *et al.*, 2012), to Winkler-based methods (e.g., Yim and Chopra, 1985; Houlsby *et al.*, 2005; Allotey and El Naggar, 2008; Raychowdhury and Hutchinson, 2009), and sophisticated macro-element modeling (e.g., Paolucci, 1997; Crémer *et al.*, 2001; Grange *et al.*, 2008; Chatzigogos *et al.*, 2009; Figini *et al.*, 2012). In all of the above cases, *experimental* simulation has been a key instrument to calibrate and validate constitutive, Winkler, and macro-element models, and to provide evidence on the mechanisms and factors affecting the response. Experimental studies can be broadly categorized in 1 g testing, either under cyclic loading [Negro *et al.*, 2000; Faccioli *et al.*, 2001] or through shaking table tests [Shirato *et al.*, 2008; Paolucci *et al.*, 2008], and centrifuge model testing [Kutter *et al.*, 2003; Gajan *et al.*, 2005; Gajan and Kutter, 2008; 2009].

As part of the ongoing EU-funded research project *DARE*, which aims at verifying the effectiveness of such emerging seismic design concepts and improving their applicability in practice, the potential effectiveness of rocking isolation has been explored analytically (through nonlinear FE analysis) for an idealized *RC* bridge pier [Anastasopoulos *et al.*, 2010a], and for simplified two-story *RC* frame structures [Gelagoti *et al.*, 2012; Kourkoulis *et al*., 2012]. In both cases, the analysis showed that rocking isolation may increase substantially the safety margins against collapse, even for seismic motions substantially exceeding the design limits, at the cost of increased permanent settlement and foundation rotation. The latter were shown to be within tolerable limits, provided that the factor of safety against vertical loads FS_v is adequately large to ensure uplifting-dominated response (see also Gajan and Kutter, 2008).

Aiming to verify the seismic performance of rocking-isolated structures, and to provide experimental evidence supporting the findings of the numerical simulations, this article investigates experimentally the seismic performance of an idealized single degree of freedom (SDOF) structure, considered representative of a bridge pier. To unravel the effectiveness of the rocking isolation concept, the physical model is founded on: (i) a conventionally designed relatively large foundation; and (ii) a smaller foundation, representative of rocking isolation. A series of shaking table tests are conducted at the Laboratory of Soil Mechanics of the National Technical University of Athens (NTUA), employing as seismic excitation real records of varying intensity. Emphasis is placed on the resistance against cumulative damage due to successive earthquakes — a commonly postulated potential drawback of the new seismic design philosophy.

2. Problem Definition

As previously mentioned, the effectiveness of rocking isolation was studied numerically in Anastasopoulos *et al.* [2010a] utilizing a simple but fairly realistic bridge pier as an illustrative example (Fig. 1). Inspired from the Hanshin Expressway Fukae section, which collapsed during the devastating 1995 Kobe earthquake (e.g., Seible *et al.*, 1995), the idealized prototype refers to a moderately tall RC bridge pier supported on a shallow square foundation of width B, sitting upon a homogenous undrained soil stratum. As sketched in Fig. 1a, two design alternatives were considered: (a) conventional capacity design, materialized through an adequately large $B = 11$ m square foundation; and (b) rocking

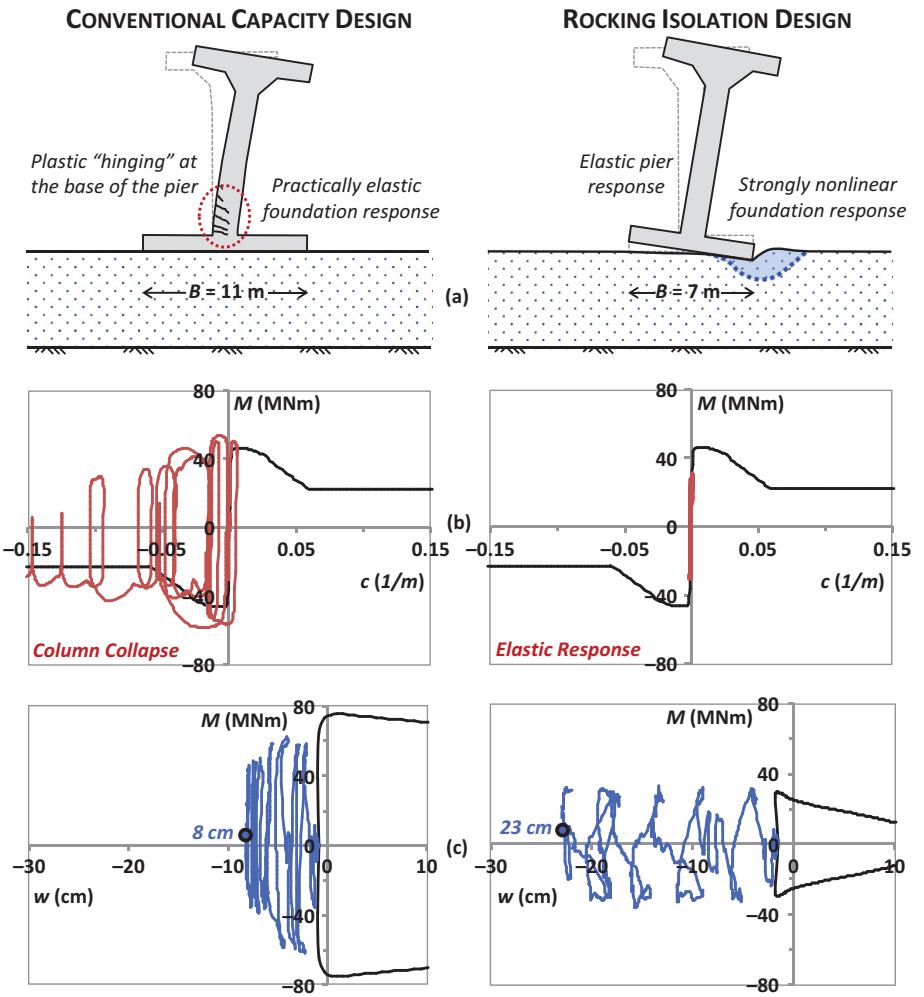

FIGURE 1 (a) Comparison of conventionally designed bridge pier (left column) with rocking isolation design (right column). Example comparison of the two design alternatives subjected to extreme seismic shaking (Takatori, Kobe 1995) for a typical bridge pier analyzed employing the finite element method [Anastasopoulos *et al.*, 2010]; (b) RC pier moment–curvature response; and (c) foundation moment–settlement response. Note that the backbone curves (black lines) have been deduced from monotonic static pushover analysis (color figure available online).

isolation design, achieved through a smaller $B = 7$ m foundation. In the case of the conventionally designed system, the moment capacity of the foundation exceeds that of the pier, guiding the plastic hinge at the base of the pier. In contrast, the moment capacity of the $B = 7$ m foundation of the rocking isolated alternative is (about 40%) lower than that of the pier, guiding plastic deformation at the soil-foundation interface.

A large number of nonlinear static and time history FE analyses were carried out by Anastasopoulos *et al.* [2010], wherein the two design alternatives were compared for various earthquake scenarios, making use of an ensemble of seismic excitations. The numerical method assumed plane-strain soil conditions accounting for material (both in the soil and the superstructure) and geometric nonlinearities (due to uplifting and P–δ effects). Results consistently indicate the superior performance of the rocking isolated alternative, especially when subjected to large intensity seismic shaking substantially exceeding the design limits (i.e., when "life safety" is the primary concern). One such comparison is summarized in Figs. 1b and c, where the performance of the two design alternatives subjected to the devastating Takatori record (Kobe, 1995) is shown in terms of moment–curvature response of the RC pier and moment–settlement response of the foundation. While the conventionally designed system appears bound to collapse, with the ductility demand overly exceeding the capacity of the RC pier, the rocking-isolated system survives such tremendous seismic shaking practically unscathed (Fig. 1b). Presumably, its superior performance is directly associated to strongly inelastic foundation response, unavoidably leading to an increase of foundation settlement (Fig. 1c).

Aiming to strengthen the validity of these findings, a very similar idealized bridge pier is utilized herein as the conceptual prototype. As illustrated in Fig. 2a, the bridge pier of height $h = 13$ m supports a bridge deck of mass $m = 1200$ Mg, founded on a square foundation of width $B = 11$ m (for the conventionally designed system) or 7 m (for the rocking isolated alternative), resting on a layer of dense sand. To focus on foundation inelastic response, no attempt was made to model the flexibility and flexural strength (i.e., the bending moment capacity) of the pier, which is considered herein elastic and relatively rigid (the fixed-base system has a dominant period $T = 0.16$ s). Hence, the earthquake-induced damage of the pier is assessed *indirectly*, through comparison of the seismic demand (i.e., the measured bending moment) with the theoretical (i.e., according to the design) moment capacity of the pier: $M_u{}^P \approx 46$ MNm (see Anastasopoulos *et al.*, 2010a). Although such estimation is definitely of approximate nature and constitutes a limitation of this study, it is considered appropriate for a first qualitative comparison of the two alternative design concepts.

The experimental model (Fig. 2b) was deduced from the conceptual prototype, making use of the scaling laws governing reduced-scale physical modeling [Muir Wood, 2004], for a linear geometric scale of $1 : 20$ ($n = 20$). The latter was chosen on the basis of the capacity of the shaking table and the internal dimensions of the soil container.

At this point, it should be noted that the stress field within the soil cannot be reproduced in reduced-scale testing, unavoidably leading to scale effects originating from the pressure-dependent behavior of soil. To compensate for these inherent shortcomings of reduced-scale testing (which can be fully alleviated only through centrifuge model testing), scale effects were accounted for in the design of the experiments, and particularly in the design of the foundation models, as described in detail in the ensuing sections.

3. Experimental Methodology

A series of reduced-scale static and dynamic tests were conducted at the Laboratory of Soil Mechanics of NTUA to comparatively assess the performance of the two design

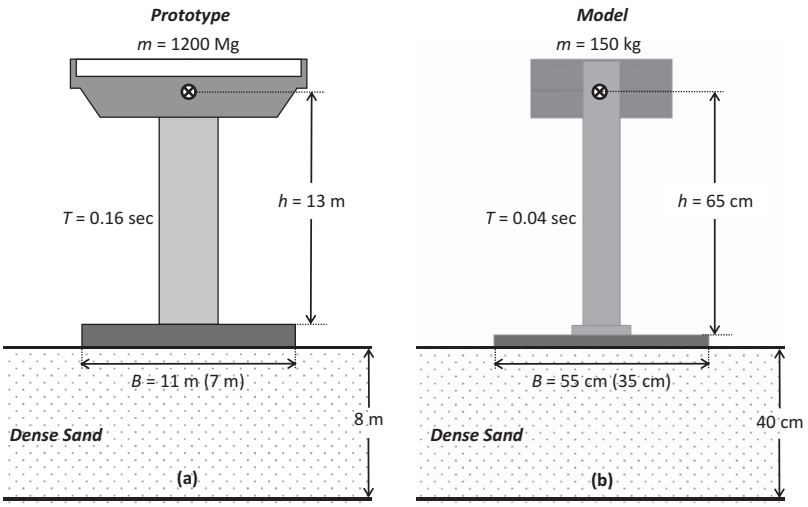

FIGURE 2 Problem definition: (a) conceptual prototype of an idealized stiff bridge pier lying on dense sand; and (b) corresponding shaking table model (in 1 : 20 scale).

alternatives. The pier models were subjected to various loading schemes. First, a series of vertical push tests were conducted to measure the bearing capacity of the two foundation systems under pure vertical loading and verify their design safety factors (FS_V). The capacity under combined N–Q–M loading was also investigated through displacement-controlled horizontal push tests. The actual "seismic" factors of safety (FS_E) were thereby calculated and compared to the theoretical values. Slow cyclic lateral push tests were also carried out, wherein loading was applied at the center of mass through displacement cycles of increasing amplitude, revealing that an overstrength mechanism takes place affecting mainly the capacity of small foundations. Finally, a series of shaking table tests were conducted studying the response of the two pier models to seismic excitations of different characteristics. Due to length restrictions, emphasis is placed on shaking table test results; the vertical and horizontal (monotonic and cyclic) push tests are discussed in detail in Drosos *et al.* [2012].

3.1. Pier–Foundation Modeling

As illustrated in Fig. 3, the foundation–structure model consists of three main parts, all made of steel: the foundation, pier, and mass (representing the deck of the bridge). It may be readily observed that instead of the square footing of the conceptual prototype, the foundation is modelled with two separate footings of width B in the direction of shaking, but of substantially smaller breadth $L/2$ in the out-of-plane direction. The reason behind this intentional discrepancy lies in the treatment of the aforementioned scale effects. Due to the scale-induced strength discrepancy between model and prototype soil, direct geometric scaling of the foundation would result to incorrect scaling (overestimation) of its capacity. Regarding foundation response, to achieve similitude between the model and the prototype, similarity has to be maintained in terms of:

(a) the ratio of the vertical load acting onto the foundation to its vertical bearing capacity : N/N_u;

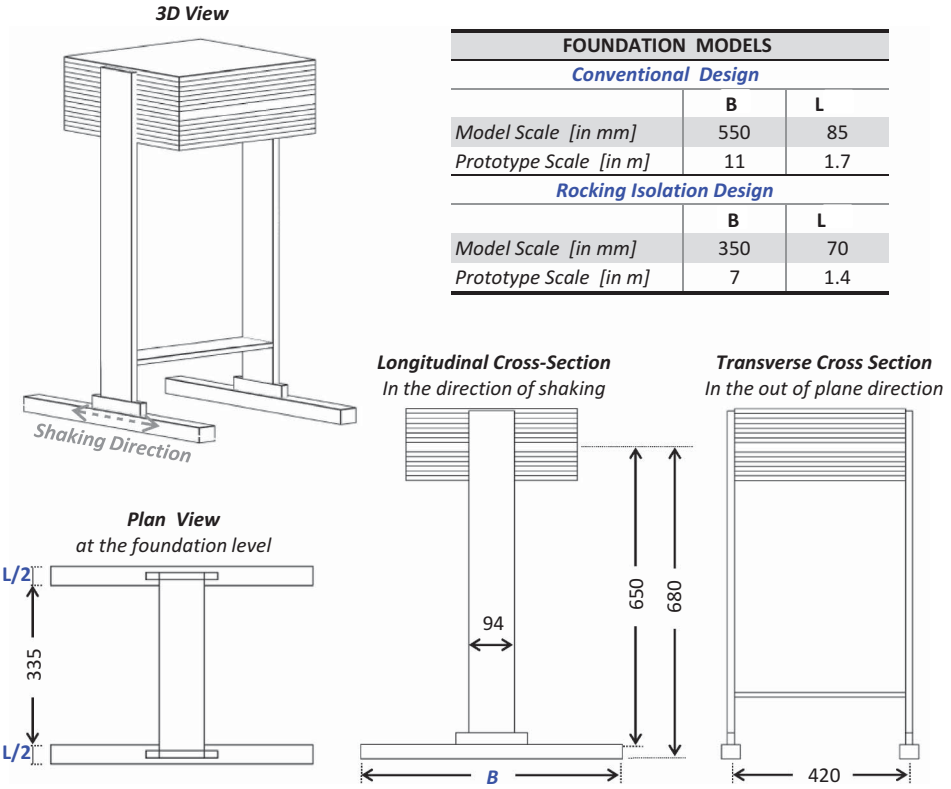

FIGURE 3 Configuration of the pier–foundation models used for the shaking table experiments (all model dimensions in [mm]) (color figure available online).

(b) the ratio of the lateral load acting onto the foundation to its lateral capacity : Q/Q_{ult}, M/M_u; and
(c) the slenderness ratio, defined here as the ratio of the height of the pier h to the foundation breadth B in the direction of shaking: h/B.

The first two conditions are satisfied by preserving the factors of safety for vertical (FS_V) and combined-seismic loading (FS_E) in the model the same as in the prototype. However, given the overestimation of soil strength due to scale effects, this can only be achieved by reducing the foundation area. But doing so in both directions would violate the requirement for preservation of the slenderness ratio h/B, which controls the rocking response. Therefore, the foundation area was reduced by decreasing only the out-of-plane foundation dimension L. The latter was calculated with respect to the intended values of FS_V and FS_E for each one of the two systems, making use of bearing capacity formulae for pure vertical loading [Meyerhof, 1951] and combined N–Q–M loading [Butterfield and Gottardi, 1994] for an average "effective" friction angle $\phi \approx 44°$. The latter was back-calculated through a series of vertical push tests on foundations of different dimensions.

The foundation design was verified by a series of vertical and horizontal pushover tests, documented in detail in Drosos *et al.* [2012]. It is important to note that, although it cannot be considered as an accurate reproduction of the prototype foundation (as it ignores

foundation shape effects), it is considered as a reasonable compromise for the key aspects of the studied problem.

For stability in the out-of-plane direction, as L ended up being much smaller than B, the deck-mass was supported through a Π shaped column-foundation system (an idea already employed by Gajan *et al.*, 2005), with the two footings of out-of-plane breadth $L/2$ placed at an adequately large distance to prevent interaction effects. The two footings were rigidly connected to the two steel columns, supporting a rigid slab positioned at height $h = 65$ cm above the foundation level (corresponding to $h = 13$ m of the prototype). The superstructure mass (consisting of 1 cm thick steel plates) was installed symmetrically above and below the rigid slab, so that the center of mass is maintained at the desired level. Sandpaper was placed underneath the foundation to achieve a realistically rough foundation-soil interface (corresponding to a coefficient of friction $\mu \approx 0.7$).

Table 1 gives an overview of the two pier models, summarizing the main dimensions and physical properties. The design seismic loads (Q and M) were calculated assuming acceleration $\alpha = 0.3$ g acting pseudo-statically at the center of mass of the deck and are presumably the same for the two piers, which have the same above-ground structural characteristics. As previously mentioned, the theoretical capacity of the two foundation systems in pure vertical loading and combined loading was estimated using well-established formulas from the literature and is shown to compare reasonably well with the results from vertical and monotonic horizontal push tests, respectively. Significantly larger is the foundation capacity under cyclically applied lateral loading, denoted in the table with an asterisk (*), due to the overstrength mechanisms discussed in detail by Drosos *et al.* [2012]. Finally, the table indicates the actual (measured) FS_E and FS_V values for the conventionally designed and the rocking-isolation alternative verifying the respective, previously described, design concept.

3.2. Model Preparation and Instrumentation

As shown in Fig. 4, the foundation-structure model was installed inside a rigid soil container 1.6 m in length, on top of a 40 cm deep dense sand stratum (corresponding to 8 m of the prototype). The model was carefully lowered on the soil surface using four mechanical jacks, so as not to disturb the soil surface. The latter consists of dense $D_r \approx 85\%$ *Longstone* sand, prepared by dry pluviation using an electronically controlled sand raining system, designed to produce samples of controllable relative density D_r . The utilized soil is an industrially produced uniform and fine quartz sand with mean grain size $d50 = 0.15$ mm and uniformity coefficient $d_{60}/d_{10} = 1.42$. The void ratios at the loosest and densest state have been measured as $e_{max} = 0.995$ and $e_{min} = 0.614$, respectively. Its properties, as derived through soil element testing, are documented in Anastasopoulos *et al.* [2010b].

Two (*Seica B1*) miniature accelerometers were embedded within the soil at 5 cm depth (corresponding to 1 m in prototype scale) to measure the acceleration directly underneath the foundation, and at a distance (Fig. 4a). After installing the two accelerometers, the pluviation continued and the soil surface was carefully levelled to allow for accurate and horizontal positioning of the model. The foundation-structure model was instrumented to allow direct recording of accelerations, flexural strains, and horizontal and vertical displacements. The latter were measured by (Space Age Series 6) miniature draw-wire and (Waycon) laser displacement transducers. The acceleration at characteristic model locations (foundation edges, deck mass) was recorded by vertical and horizontal accelerometers (of the same type). Strain gauges installed at the base of the steel piers were used to measure bending strains, used as a more direct measurement of the bending moment at the base of

TABLE 1 Summary of the two foundation systems geometry, capacity, and design characteristics (in prototype scale)

Foundation design CONCEPT :		Conventional	Rocking Isolation
	Dimensions		
Length	**B (m)**	11	7
Width	**L (m)**	1.7	1.4
Slenderness ratio	**h/B**	1.2	1.9
Fix. base Period	$\mathbf{T^0}$ **(s)**	0.16	0.16
Flex. base Period	$\mathbf{T^{SSI}}$ **(s)**	0.47	0.72
	Static Loads		
Deck Mass	**m (Mgr)**	1200	1200
Total Weight	**N (MN)**	14.4	13.6
	Dynamic Properties		
Fix. base Period	$\mathbf{T^0}$ **(s)**	0.16	0.16
Flex. base Period	$\mathbf{T^{SSI}}$ **(s)**	0.47	0.72
	Seismic Design Loads (assuming $A_E = 0.24$ g, $\alpha = 0.3$ g for $q = 2$)		
Shear	**Q (MN)**	3.5	3.5
Moment	**M (MN)**	48	48
	Theoretical Ultimate Capacity ($\phi = 44°$)		
Vertical	$\mathbf{N_u}$ **(MN)**	104.2	44.6
Combined Lateral	$\mathbf{Q_u}$ **(MN)**	3.8	1.9
	$\mathbf{M_u}$ **(MN)**	51.7	26.4
	Measured Ultimate Capacity		
Vertical	$\mathbf{N_u}$ **(MN)**	98.8	44.4
Combined Lateral	$\mathbf{Q_u}$ **(MN)**	4.3 (4.7*)	1.8 (2.3*)
	$\mathbf{M_u}$ **(MN)**	59 (64*)	25 (31*)
	(Actual) Factors of Safety		
Static	$\mathbf{FS_V}$	6.9	3.3
Seismic	$\mathbf{FS_E}$	1.2	0.7

* : maximum capacity measured during cyclic lateral push tests [Drosos et al., 2012] where overstrength was observed.

the pier (in addition to the *indirect* measurement, based on acceleration of the deck-mass). A photo of the model with the smaller $B = 7$ m foundation (rocking isolation design) is shown in Fig. 4b.

3.3. Shaking Table Testing Sequence

Figure 5 presents the seismic motions used as base excitation in the shaking table tests. Being selected so as to represent motions of various characteristics and intensities, this ensemble of acceleration time histories involves both real records and artificial motions. Focusing on real seismic records, Fig. 6 portrays the elastic acceleration response spectra

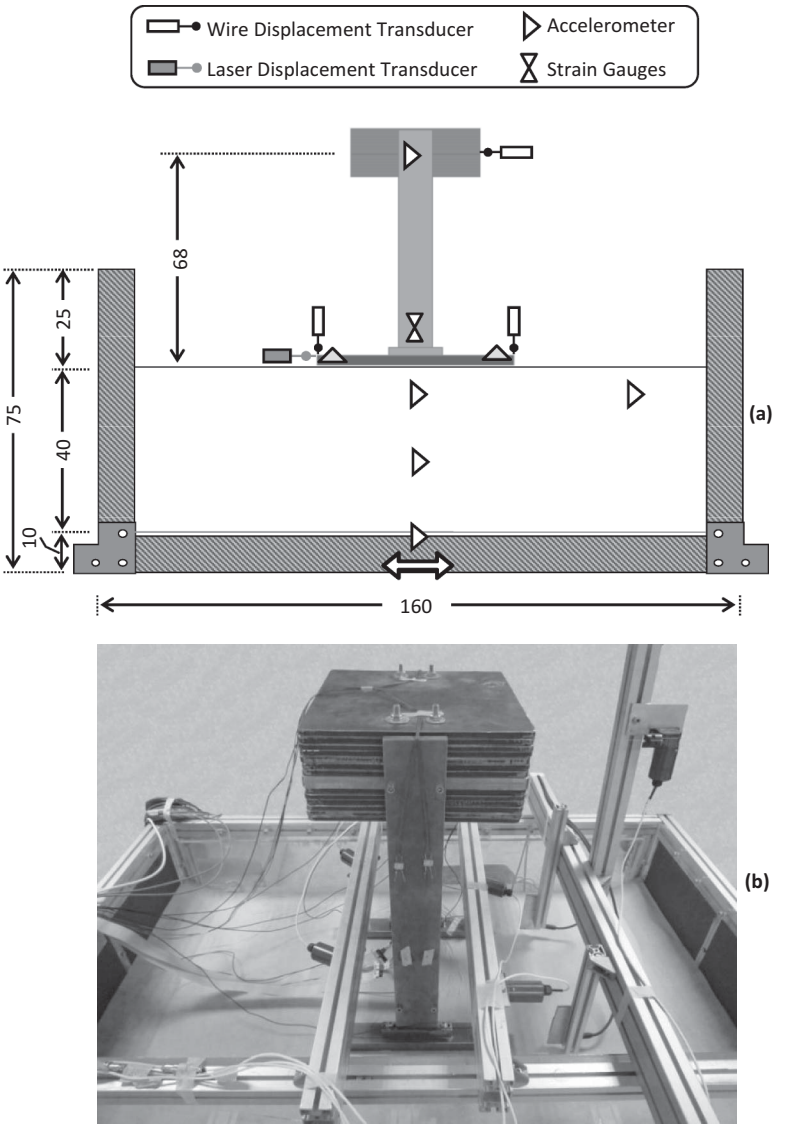

FIGURE 4 Set up of shaking table experiments: (a) schematic illustration of model and instrumentation with dimensions in [mm]; and (b) photo of the model (with $B = 7$ m foundation) prior to shaking.

of the theoretical (target) input motion in comparison with the motion measured at the base of the model. The difference between the two, being of considerable magnitude in the relatively high frequency range, is the result of limitations in the motion reproduction efficiency of the shaking table. Furthermore, comparison of the excitation response spectrum with the design spectrum (grey line) indicates the relative to the design earthquake intensity, revealing that the test series covers a wide variety of earthquake scenarios, spanning from medium intensity excitations comparable to the design earthquake (i.e., the Aegion record) to very strong seismic motions that dramatically exceed the design (such as the Rinaldi and Takatori records).

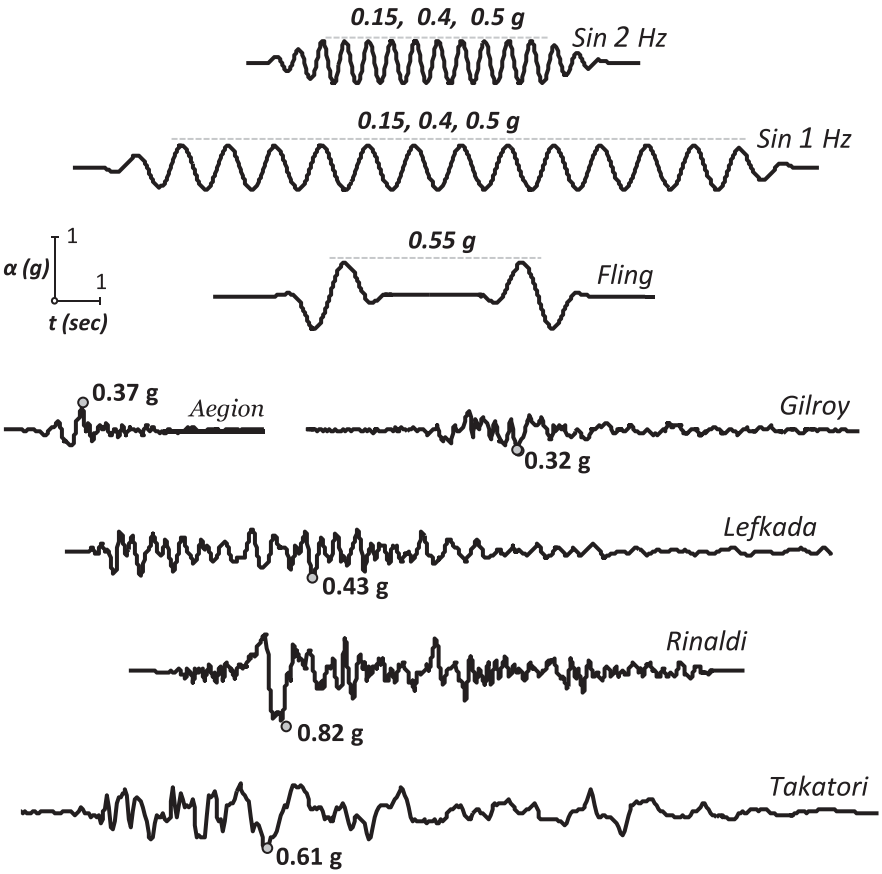

FIGURE 5 Real records and artificial motions used as seismic "bedrock" excitation in the shaking table tests.

As summarized in Table 2, three different shaking sequences were simulated, each one of them conducted using a new model (i.e., six different models were tested in total). In *Sequence 1*, the model was first subjected to artificial multi-cycle sinusoidal motions of progressively increasing intensity, followed by a sequence of real records of varying intensities, and an artificial fling-type motion. *Sequence 2* started with real records in an ascending order of intensity — starting with the Aegion record and ending up with the devastating directivity-affected Rinaldi and Takatori records, followed by artificial (fling and sinusoidal) motions. Finally, *Sequence 3* (conducted only for the rocking isolated system) started with the Takatori record in order to investigate the performance under very strong seismic shaking, when the soil has not been disturbed by previous seismic excitations.

4. Comparative Performance Assessment

Focusing on real records, characteristic examples are discussed being representative of: (a) moderate seismic shaking not exceeding the design; (b) strong seismic shaking slightly exceeding the design; and (c) extreme seismic shaking substantially exceeding the design. This way, the performance of the two design alternatives is comparatively assessed for

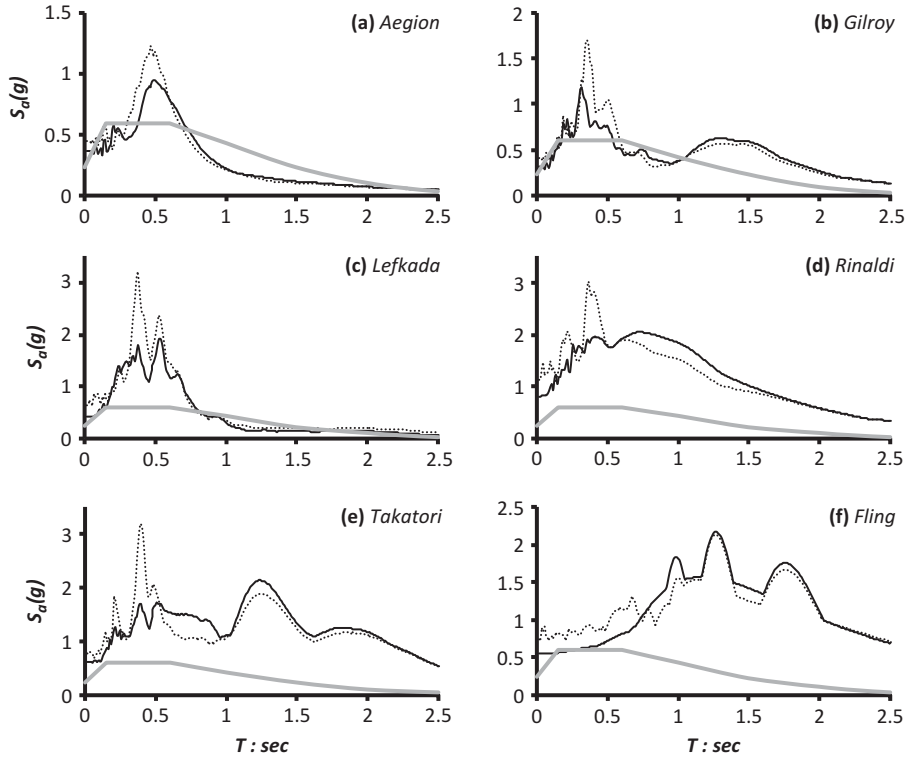

FIGURE 6 Theoretical (target) and measured (shaking table system output) elastic ($\xi = 5\%$) acceleration response spectra of the real earthquake excitations and the fling-step pulse used in the shaking table tests are compared with the design spectrum.

TABLE 2 The three seismic shaking sequences of the shaking table tests

Sequence 1		Sequence 2		Sequence 3	
Excitation	α_{max} (g)	Excitation	α_{max} (g)	Excitation	α_{max} (g)
Sin - 2 Hz	0.15	Aegion	0.37	***Takatori***	***0.61***
	0.40	Lefkada	0.43	Fling	0.55
	0.50	Gilroy	0.32	Sin - 2 Hz	0.5
Sin - 1 Hz	0.15	Rinaldi	0.82	Sin - 1 Hz	0.5
	0.40	***Takatori***	***0.61***		
	0.50	Fling	0.55		
Takatori	***0.61***	Sin - 2 Hz	0.50		
Aegion	0.37	Sin - 1 Hz	0.50		
Lefkada	0.43	Sin - 1 Hz	1.00		
Gilroy	0.32				
Rinaldi	0.82				
Fling	0.55				

different levels of seismic shaking, corresponding to earthquake scenarios of different probability of occurrence (or return period). The performance of the two systems subjected to sinusoidal motions is discussed in Drosos *et al.* [2012], along with the detailed results of monotonic and cyclic pushover tests. Unless otherwise stated, in the sequel the results are presented in prototype scale. All of the results presented in this section refer to shaking *Sequence 2* (i.e., starting with real records).

4.1. Moderate Seismic Shaking Not Exceeding the Design

The record from the 1995 M_s 6.2 Aegion (Greece) earthquake can be considered as a moderate intensity seismic excitation. Although its elastic response spectrum exceeds the design spectrum for the range of periods between 0.4 and 0.8 s (Fig. 6a), due to its characteristically short duration and the presence of (practically) a single strong motion pulse of moderate acceleration amplitude (0.37 g), it is reasonably considered as a seismic motion within the limits of the design.

Figure 7 compares the performance of the two design alternatives in terms of time histories of deck acceleration (i.e., at the mass of the SDOF oscillator). A critical acceleration α_c can be defined as the maximum acceleration that can possibly develop at the deck mass. Since the maximum moment at the soil-foundation interface cannot exceed the moment capacity of the foundation M_u, the critical acceleration will be $\alpha_c = M_u/mgh$. In view of its measured moment capacity (see Table 1) the large conventionally designed $B = 11$ m foundation can sustain $\alpha_c \approx 0.37$ g, or 0.40 g taking account of the observed cyclic overstrength. Due to its subantially lower moment capacity, the smaller $B = 7$ m foundation of the rocking-isolated system can sustain substantially lower acceleration: $\alpha_c \approx 0.16$ g, going up to 0.20 g, if cyclic overstrength is accounted for.

Interestingly, in this excitation event the measured acceleration is in both cases quite lower than the corresponding α_c value, implying that none of the two foundations reached its ultimate moment capacity. Yet, the response of both systems deviates substantially from the linear-elastic regime, demonstrating non negligible hysteretic material behavior especially under the effect of the single strong motion cycle (see the M–θ loops of Fig. 8). Thus, nonlinear soil–structure interaction (*SSI*) takes place to drastically modify the response in comparison to pure elastic conditions, causing in this case considerable attenuation of the input motion. A rough outline of this effect is attempted in Fig. 9, where the transient stiffness degradation during seismic loading may be traced in the load-displacement (P–δ) response of both pier systems (Fig. 9a) and related to the dynamic amplification/attenuation response of an equivalent SDOF oscillator. Figure 9b illustrates the acceleration response spectra of the surface earthquake motion for a range of damping ratios ($\xi = 5, 10, 15, 20\%$) highlighting the spectral ordinates that correspond to oscillation on a fixed base (T^0), oscillation on a flexible base assuming elastic soil–structure interaction ($T^{SSI,lin}$), and nonlinear soil-structure interaction at the increment of maximum deck displacement ($T^{SSI,nl}$).

Even under the assumption of elasticity, SSI results in significant increase of the natural period of the two systems in comparison to the fixed base period of 0.16 s, this increase being presumably unequal for the two piers owing to their different foundations (note that the system on conventionally designed foundation is more than two times stiffer than the rocking isolated alternative). Interestingly, thanks to its increased flexibility, the rocking isolated system responds off the range of "resonance" for the specific excitation while, by contrast, the effect of SSI is much less favorable for the conventional system, the natural period of which coincides with the dominant period of excitation implying significant spectral amplification (Fig. 9b). Yet, the actually nonlinear rocking response causes further increase in the effective period of response so much as to lead to attenuation of motion

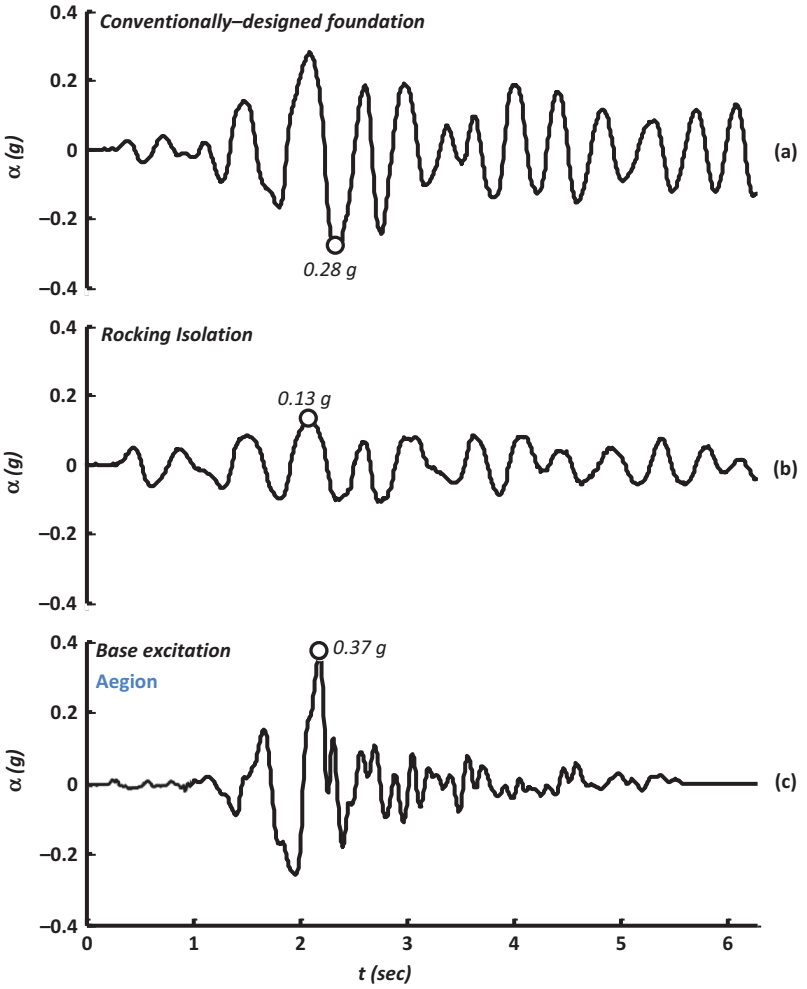

FIGURE 7 Deck acceleration time histories for *moderate* seismic shaking (Aegion): (a) system on conventionally designed $B = 11$ m foundation, compared to (b) rocking isolated alternative with under-designed (to promote uplifting) $B = 7$ m foundation; (c) base excitation (color figure available online).

even for the conventional system. It is worth noting that the secant stiffness and period of the two systems at the increment of maximum deck displacement ($K^{SSI,nl}$ and $T^{SSI,nl}$) correspond to spectral accelerations of around 0.3 g for the conventional and 0.16 g for the rocking-isolated system (for a reasonable estimate of the damping ratio of 15% and 20%, respectively) which are in surprisingly good agreement with the respective maximum deck acceleration recordings of Fig. 7.

Due to its frequency content, this seismic excitation is expected to have a relatively stronger effect on the conventional system, the natural period of which is very close to the dominant period of the excitation, than the more flexible rocking isolated pier. Hence, despite having about two times greater bearing capacity, the large conventionally designed foundation suffers almost the same amount of shaking-induced settlement ($\approx$ 3 cm) with the quite smaller foundation of the rocking isolated pier, as evidenced by

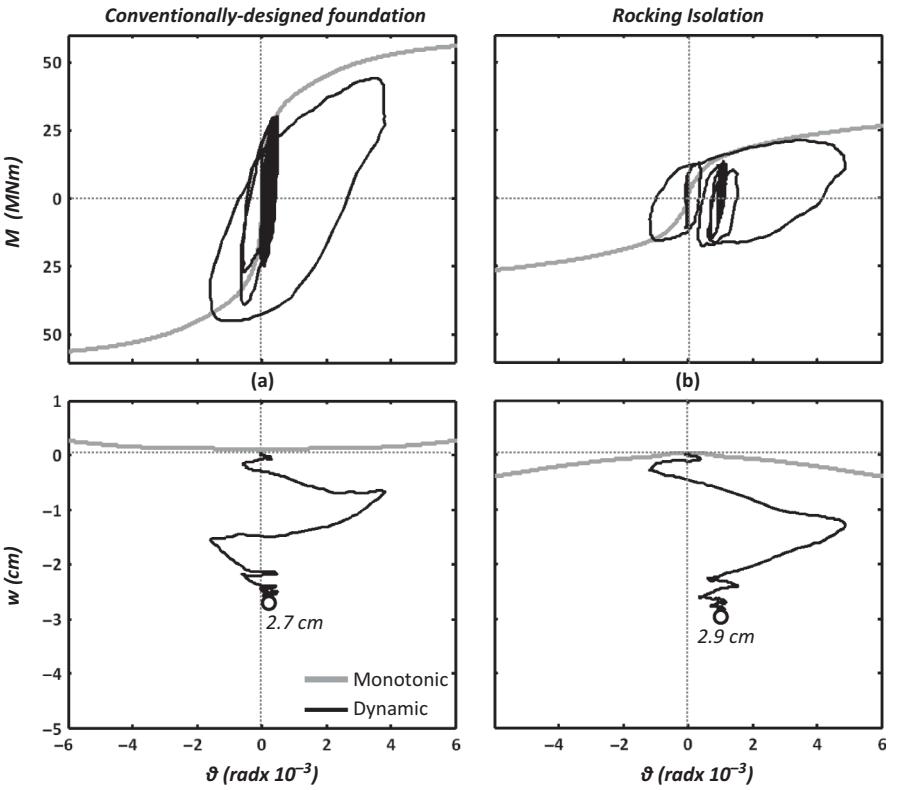

FIGURE 8 Foundation performance for *moderate* seismic shaking (Aegion). Moment–rotation ($M-\theta$) and settlement–rotation ($w-\theta$) response for: (a) system on conventionally designed $B = 11$ m foundation, compared to (b) rocking isolated alternative with under-designed $B = 7$ m foundation.

the settlement–rotation (w–θ) loops of Fig. 8. Even so, thanks to its $FS_V = 6.9$ the response of the conventional $B = 11$ m foundation is *uplifting-dominated*: observe in Fig. 8a the ascending slope of the motononic w–θ curve, which implies that the foundation midpoint tends to move upwards with increasing imposed rotation. By contrast, the smaller $B = 7$ m foundation of the *rocking-isolated* system, having a substantially lower $FS_V = 3.3$ exhibits *sinking-dominated* response: the center of the footing moves downwards (Fig. 8b).

Deck drift can be seen as an equally illustrative index of seismic performance. The total deck drift δ (i.e., the total lateral displacement of the deck) comprises three components: (a) the lateral swaying (sliding) displacement u; (b) the additional lateral displacement due to foundation rotation δ_θ; and (c) the lateral displacement due to flexural deformation of the pier δ_c. In the case examined herein, since the pier is practically rigid δ_c can be ignored. Figure 10 compares the performance of the two design alternatives in terms of total drift time histories, decoupled into the u and δ_θ components. As expected, owing to the slenderness of both systems, swaying plays a secondary role compared to rocking. The two systems experience approximately the same maximum drift $\delta \approx 8$ cm. However, in the case of the conventionally designed system the lateral deformation is fully recovered, resulting to practically zero permanent drift. The rocking-isolated system appears to retain some very limited permanent drift (≈ 2 cm), which is associated to residual foundation

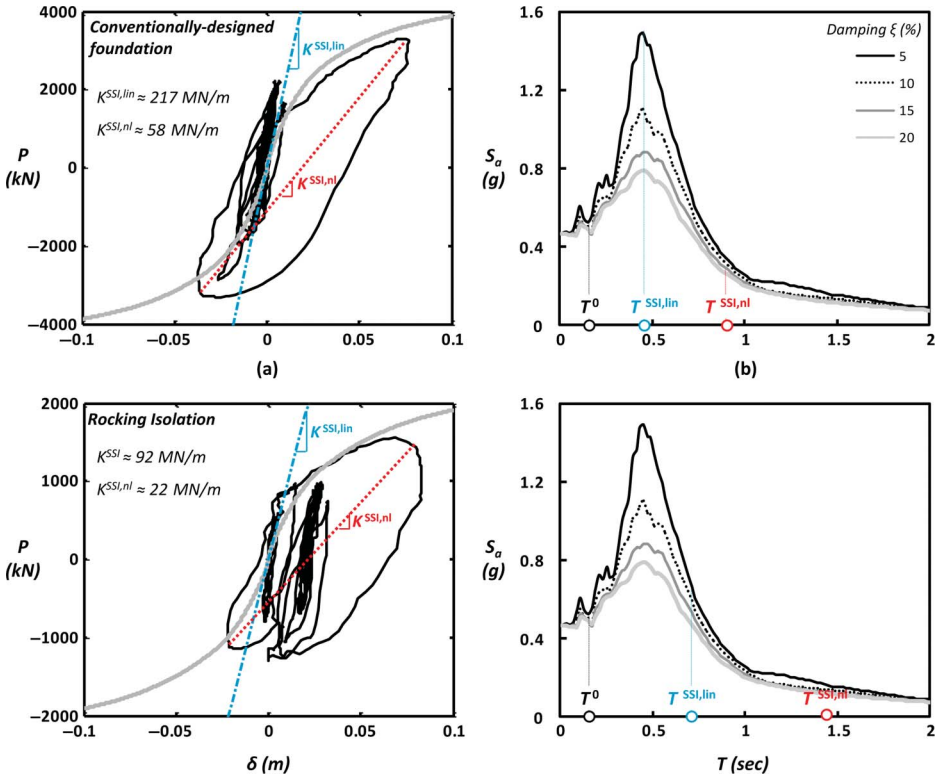

FIGURE 9 Soil structure interaction (SSI) effect on the dynamic properties of the two bridge piers for the case of excitation with the Aegion record (moderate intensity): (a) load displacement response curves indicating the initial elastic stiffness of the system ($K^{\mathrm{SSI,lin}}$) and the secant stiffness at the increment of maximum deck displacement ($K^{\mathrm{SSI,nl}}$); and (b) response spectrum of the soil surface motion highlighting the spectral ordinates corresponding to fixed base conditions (T^0), response on flexible base with elastic SSI ($T^{\mathrm{SSI,lin}}$), and nonlinear response at the increment of maximum deck displacement ($T^{\mathrm{SSI,nl}}$) (color figure available online).

rotation. Nevertheless, such a minor residual drift, yielding a drift ratio $\delta/h \approx 0.15$ %, is considered tolerable.

4.2. Strong Seismic Shaking Slightly Exceeding the Design

The Gilroy record from the 1989 M_s 7.1 Loma Prieta earthquake is utilized as an example of relatively strong seismic shaking, slightly exceeding the design (Fig. 6b). As in the previous case, the response of the two design alternatives is comparatively assessed in Figs. 11–13 in terms of deck acceleration time histories, foundation M–θ and w–θ response, and time histories of deck drift.

Time histories of deck acceleration of the two systems are compared in Fig. 11. The increase of seismic demand has a marked effect on the response of both systems, which now clearly mobilize their ultimate moment capacity as evidenced by the acceleration cut-off at 0.40 g for the conventionally designed foundation (Fig. 11a), and at 0.19 g for the

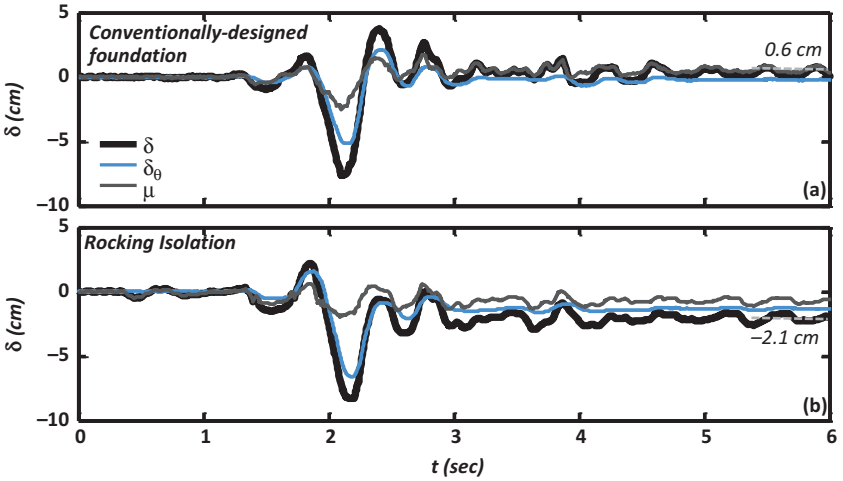

FIGURE 10 Time histories of deck drift δ, due to foundation rotation δ_θ, and swaying displacement u, for *moderate* seismic shaking (Aegion): (a) system on conventionally designed $B = 11$ m foundation, compared to (b) rocking isolated alternative with under-designed $B = 7$ m foundation (color figure available online).

rocking-isolation alternative (Fig. 11b). Both values are in very good agreement with the previously discussed α_c estimates (on the basis of monotonic and cyclic pushover tests).

These observations are confirmed by the M–θ loops of Fig. 12. The larger conventionally designed foundation reaches its ultimate moment capacity, but without exhibiting substantial nonlinearity (Fig. 12a). In stark contrast, the smaller foundation of the rocking-isolated system experiences strongly nonlinear response, as evidenced by its oval-shaped M–θ loops. As a result (and as it would be expected), the conventional system experiences substantially lower rotation compared to the rocking-isolated system. As evidenced by the w–θ curves, the larger foundation demonstrates uplifting-dominated response (observe the very steep edges of the corresponding loops) resulting in minor residual settlement of merely 1.1 cm. Contrarily, the smaller foundation of the rocking-isolated system moves downwards upon each cycle of rotation, accumulating about three times larger settlement (3.2 cm).

However, the superior performance of the larger foundation (with respect to permanent displacements) is unavoidably associated with the development of larger inertia forces. While for the rocking-isolated system the bending moment that develops at the base of the pier is bounded by the inferior moment capacity of the footing ($M_u \approx 30$ MNm), in the case of the conventionally designed foundation a moment of roughly 60 MNm is allowed to develop, substantially exceeding the capacity of the RC pier ($M_u{}^P \approx 46$ MNm). In reality, this would be associated with flexural cracking at the base of the pier, and its survival (or collapse) would be a function of the ratio of ductility demand to ductility capacity.

The larger rotation of the smaller foundation is also reflected in the time histories of deck drift (Fig. 13b). The rocking-isolated system experiences substantially larger maximum deck drift $\delta \approx 10$ cm, as opposed to roughly 6 cm of the conventional system. Interestingly, thanks to the inherent self-centering mechanism of rocking, the residual deck drift is limited to 2.4 cm (instead of 1.9 cm of the conventional system) — a value that can easily be considered tolerable. In reality, however, the system on conventionally designed foundation would be subjected to bending failure, unavoidably experiencing

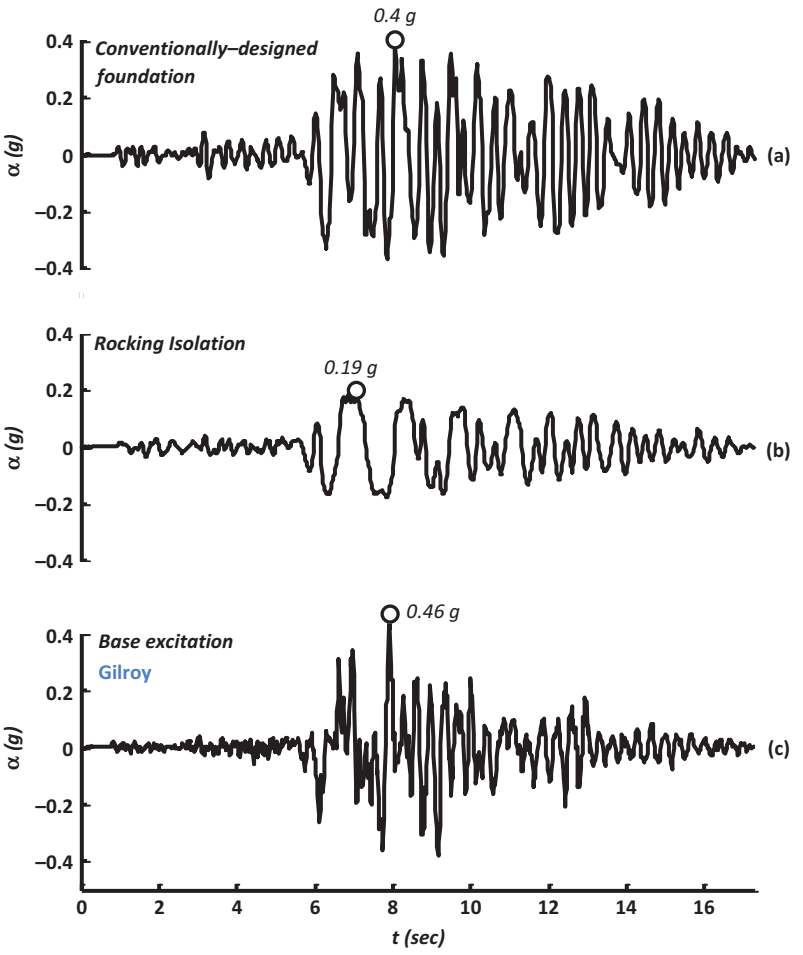

FIGURE 11 Deck acceleration time histories for *strong* seismic shaking (Gilroy): (a) system on conventionally designed $B = 11$ m foundation, compared to (b) rocking isolated alternative with under-designed (to promote uplifting) $B = 7$ m foundation; (c) base excitation (color figure available online).

additional permanent drift due to plastic flexural distortion. Although the extent of such additional deformation cannot be quantified, on the basis of numerical analysis results [Anastasopoulos *et al.*, 2010a] it is almost certain that the comparison would be largely in favor of the rocking-isolated alternative had the inelastic response of the RC pier been taken into account.

4.3. Extreme Seismic Shaking Substantially Exceeding the Design

The Rinaldi record from the devastating 1994 M_s 6.7 Northridge earthquake is utilized herein as an illustrative example of very strong seismic shaking, substantially exceeding the design limits. Containing a well-distinguished, long-duration asymmetric acceleration pulse of 0.82 g (being the result of forward-rupture directivity effects), it generates an elastic response spectrum overly exceeding the design throughout the entire period range (see

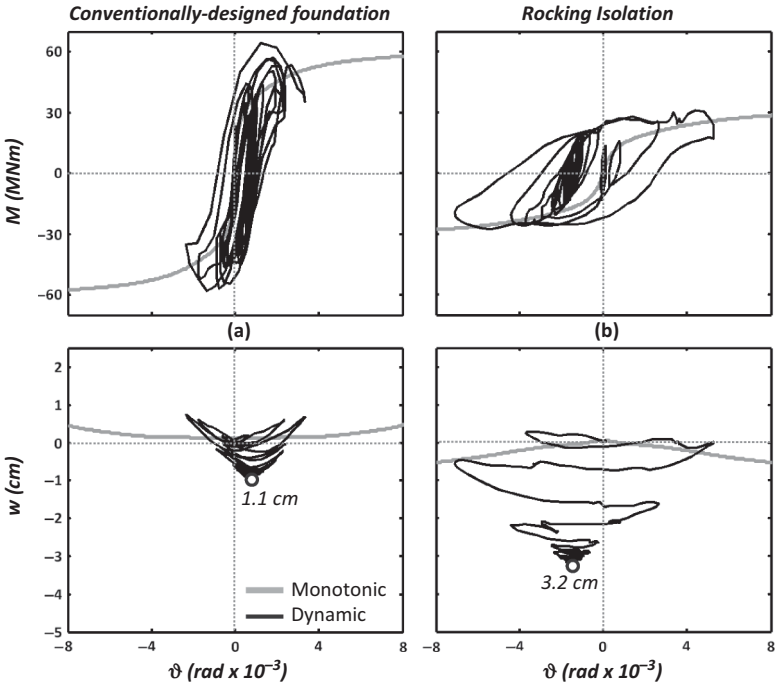

FIGURE 12 Foundation performance for *strong* seismic shaking (Gilroy). Moment–rotation ($M-\theta$) and settlement–rotation ($w-\theta$) response for: (a) system on conventionally designed $B = 11$ m foundation, compared to (b) rocking isolated alternative with under-designed $B = 7$ m foundation.

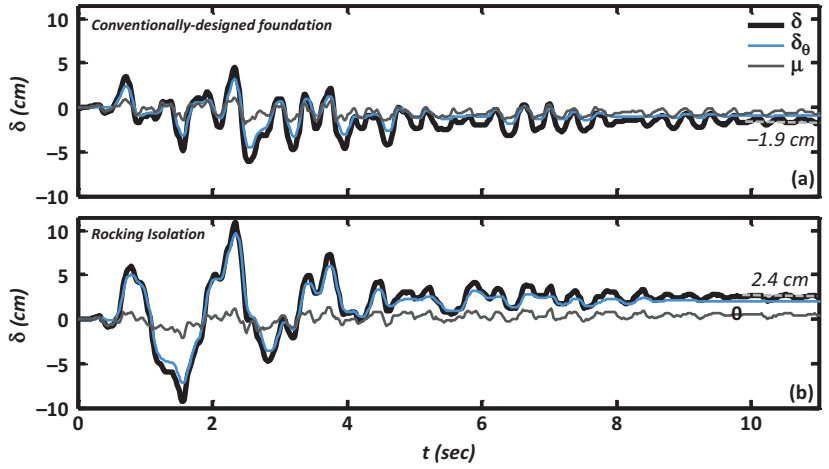

FIGURE 13 Time histories of deck drift δ, due to foundation rotation δ_θ, and swaying displacement u, for *strong* seismic shaking (Gilroy): (a) system on conventionally designed $B = 11$ m foundation, compared to (b) rocking isolated alternative with under-designed $B = 7$ m foundation (color figure available online).

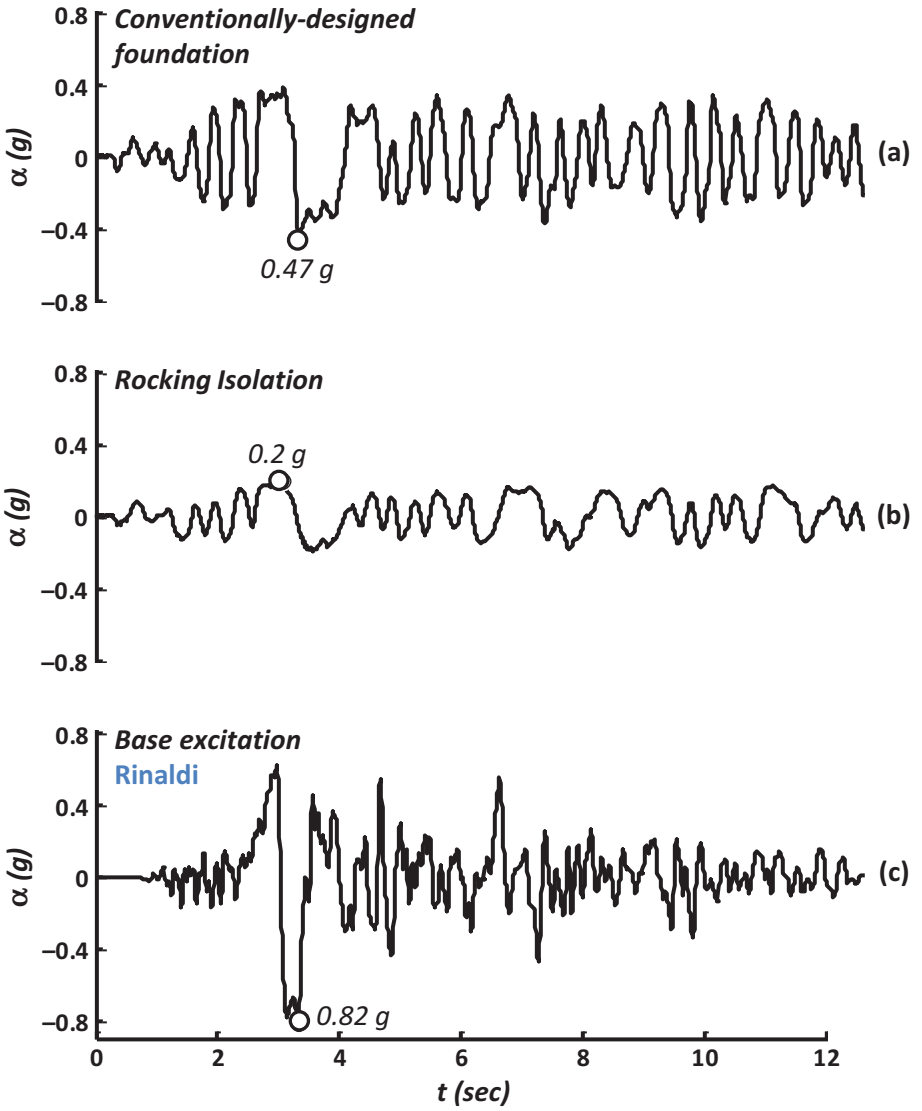

FIGURE 14 Deck acceleration time histories for *extreme* seismic shaking (Rinaldi): (a) system on conventionally designed $B = 11$ m foundation, compared to (b) rocking isolated alternative with under-designed (to promote uplifting) $B = 7$ m foundation; (c) base excitation (color figure available online).

Fig. 6d). As for the previous cases, the performance of the two design alternatives is comparatively assessed in Figs. 14–16 in terms of deck acceleration time histories, foundation M–θ and w–θ response, and time histories of deck drift.

Conspicuously nonlinear foundation response is evidenced by the time histories of deck acceleration (Fig. 14). Both systems fully mobilize their ultimate moment capacity, leading to a distinct acceleration cutoff at 0.47 g for the system on conventionally designed foundation (Fig. 14a) and at 0.2 g for the rocking-isolation alternative (Fig. 14b). In the latter case, the cutoff is in full accord with the previously discussed α_c estimate.

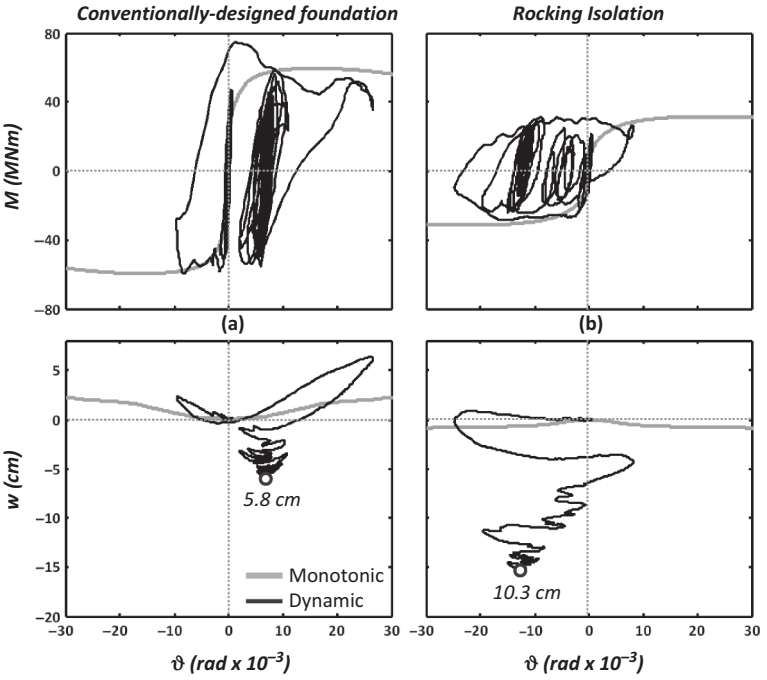

FIGURE 15 Foundation performance for *extreme* seismic shaking (Rinaldi). Moment–rotation ($M-\theta$) and settlement–rotation ($w-\theta$) response for: (a) system on conventionally designed $B = 11$ m foundation, compared to (b) rocking isolated alternative with under-designed $B = 7$ m foundation.

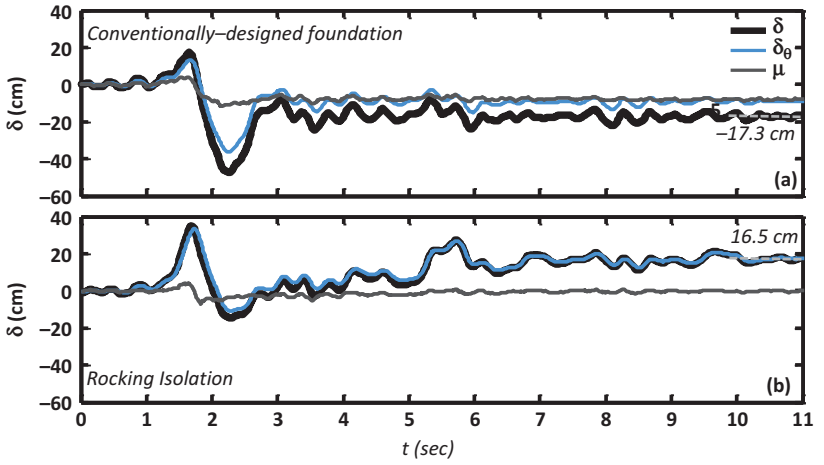

FIGURE 16 Time histories of deck drift δ, due to foundation rotation δ_θ, and swaying displacement u, for *extreme* seismic shaking (Rinaldi): (a) system on conventionally designed $B = 11$ m foundation, compared to (b) rocking isolated alternative with under-designed $B = 7$ m foundation (color figure available online).

However, the conventional system develops larger acceleration compared to the α_c estimate (0.40 g). Such performance amelioration can only be associated with soil densification during repeated seismic excitations. Observe in Table 2 that when the model was finally excited with the Rinaldi record it had already sustained four other seismic excitations. As it will be discussed in the sequel, the third shaking sequence was conducted to clarify such phenomena.

The M–θ loops of Fig. 15 confirm the strongly nonlinear response of both foundations. In contrast to the previous case (Gilroy), the maximum foundation rotation of the two design alternatives is quite similar, despite their substantial differences in terms of moment. As expected, the system on conventionally designed foundation experiences lower residual rotation compared to the rocking-isolation alternative. The residual settlement is now substantially larger for both foundations. The larger conventionally designed foundation exhibits uplifting-dominated response (enhanced by the previously discussed densification from preceding shaking events), reaching an impressive 6 cm lift-off during the strong motion cycle, and acquiring only a few millimeters of settlement by the end of it, finally accumulating 5.8 cm of settlement (Fig. 15a) as opposed to 10.3 cm of the rocking-isolated system (Fig. 15b). As for the previous case, the superior performance of the larger foundation is unavoidably associated with the development of inertia forces (of the order of 70 MNm) substantially exceeding the bending moment capacity of the pier (46 MNm). Hence, in reality the system on conventionally designed foundation would suffer substantial damage (if not collapse).

Quite interestingly, the stronger conventionally designed foundation experiences larger deck drift $\delta \approx 50$ cm as opposed to less than 35 cm of the rocking-isolation alternative (Fig. 16). Although the differences are less pronounced, the same observation holds true for the residual drift: 17.3 cm instead of 16.5 of the weaker foundation. It should be noted once again that, in reality, the system on conventionally designed foundation would experience additional permanent drift due to unavoidable flexural plastic distortion. In fact, Fig. 16a provides a very non conservative estimate of the permanent deck drift of the conventional system. Hence, it may be argued that the performance of the rocking-isolated system would be even more superior in reality, with the previously discussed settlement increase being its only real drawback.

5. Damage Accumulation and Strength Degradation

Modern seismic codes demand adequate ductility to be provided at specific locations where flexural plastic hinges are expected to form, aiming at enabling safe accommodation of inelastic strains, providing energy dissipation mechanisms, and avoiding brittle modes of failure associated with excessive strength degradation. For this purpose, strict reinforcement detailing of RC columns is required. Yet, laboratory testing of concrete elements has indicated rapid loss of strength just after the consumption of ductility capacity, and significant cyclic deterioration in the hysteretic response, especially when behavior is influenced by shear (see, for instance: Chai *et al.*, 1991; Priestley and Seible, 1995; Lehman and Moehle, 1998; Sezen, 2002). In stark contrast, rocking on compliant soil has been shown to be highly ductile, not being associated with strength degradation [Gajan and Kutter, 2008; Anastasopoulos *et al.*, 2010a].

In this section, the performance of the two design alternatives is comparatively assessed in terms of cumulative damage and strength degradation, with respect to the capacity of the respective plastic hinges (at the base of the pier or at the soil–foundation interface). As previously mentioned, the experimental simulation presented herein has not directly accounted for inelastic pier response. Therefore, an illustrative example from the

literature is utilized as the conventional design reference. It refers to a well-confined $h = 2.4$ m RC bridge pier, having a circular cross-section of 0.6 m in diameter, designed according to modern standards and having a displacement ductility capacity $\mu_\Delta \approx 6$ [Lehman and Moehle, 1998]. This large-scale RC pier model has been extensively tested to cyclic loading, and is thus considered as an appropriate example.

The comparison of the two design alternatives is portrayed in Fig. 17, in terms of strength deterioration ratio P/P_{ult} (where P is the developing load at the deck level, and P_{ult} the maximum lateral load capacity) with respect to the drift ratio δ/h. The performance of the conventional system, based on the previously discussed large-scale tests of Lehman and Moehle [1998], is depicted in Fig. 17a along with the level of damage that was observed at characteristic increments of testing. Yielding of the longitudinal reinforcement took place at $\delta/h = 1.2\%$. The RC section behaved nonlinearly at larger imposed displacements, with spalling of concrete observed at $\delta/h = 2.5$ %, followed by complete loss of the concrete cover and full exposition of the reinforcement at $\delta/h = 4\%$. At this point, the ductility capacity of the RC section is reached, and further cyclic loading results to an apparent strength degradation due to buckling of reinforcement (observed at $\delta/h = 5.5$ %). Column failure is imminent at this stage, as continued cyclic loading up to the same lateral displacement causes fracture of longitudinal reinforcement and a rather pronounced degradation of the lateral capacity: $P/P_{ult} \approx 0.5$.

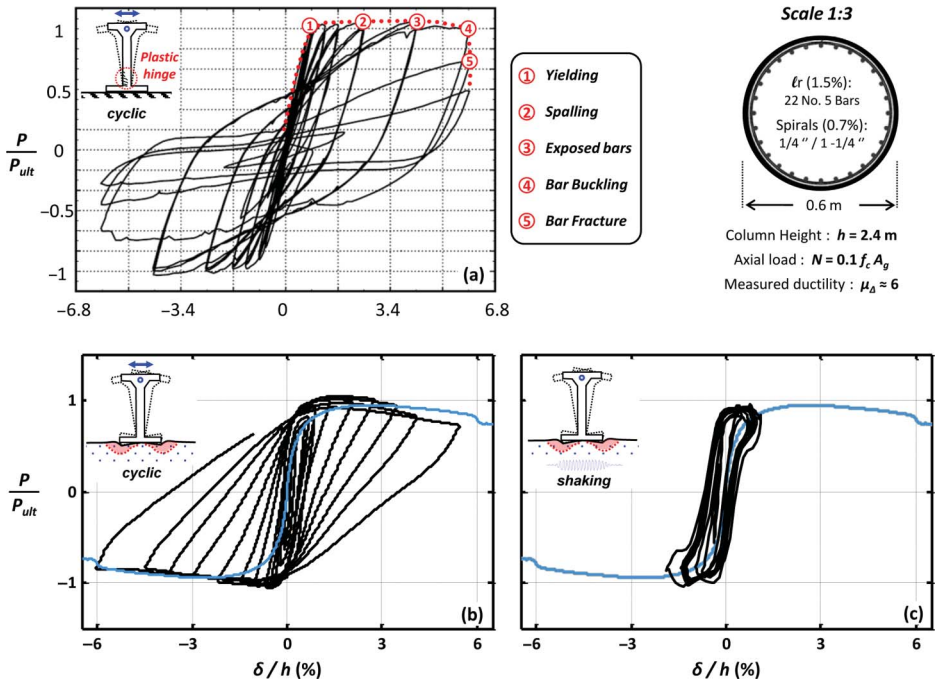

FIGURE 17 Comparative performance assessment in terms of cumulative damage capacity. Strength deterioration ratio P/Pu (i.e., lateral load at the deck divided by the capacity) with respect to the drift ratio δ/h: (a) conventionally designed, well reinforced (according to modern seismic codes), RC pier subjected to cyclic loading up to failure (after Lehman and Moehle, 1998), compared to the rocking isolated pier of this study subjected to (b) cyclic loading; and (c) shaking table testing with a 12-Cycle low-period sinusoidal excitation of 0.5 g (Sin 1Hz @ 0.5 g) (color figure available online).

The performance of the rocking-isolated system subjected to displacement-controlled cyclic pushover testing is portrayed in Fig. 17b. Being remarkably resistant to cumulative cyclic loading, the system does not suffer any evident loss of strength after being subjected to 10 cycles of progressively increasing lateral displacement, up to $\delta/h = 3.5\%$. Further increase of the cyclic displacement amplitude to $\delta/h = 4\%$ and finally to 5.6% leads to limited strength degradation, not exceeding 25%: $P/P_{ult} \approx 0.75$. This can be considered as a noteworthy advantage compared to the abrupt strength degradation observed in the case of the conventional system: $P/P_{ult} < 0.5$ for almost the same drift ratio. Even more important is the recognition that in the case of the rocking-isolated system, the observed strength degradation is mainly related to P–δ effects, rather than accumulation of damage in the "plastic hinge." Therefore, it can be argued that the lateral capacity of the rocking-isolated system will keep degrading at the same rate with increasing imposed displacement, without exhibiting any rapid strength degradation. Overturning collapse will finally take place at much larger displacement.

Demonstrating such a profoundly more ductile failure mechanism in comparison to conventional design, and furthermore, such "immunity" to cyclic strain accumulation, the rocking-isolated system can be claimed to offer increased safety margins against collapse. This is further confirmed in Fig. 17c, which depicts the performance of the rocking-isolated system subjected to a 12-cycle 1 Hz sinusoidal motion of $PGA = 0.5$ g.

6. Performance in Successive Earthquakes

Another commonly postulated potential drawback of rocking isolation is related to the risk of damage accumulation in successive seismic events. Although the performance of a rocking-isolated structure may be advantageous, after sustaining a strong earthquake the damage to the system will be in the form of permanent deformation: settlement and rotation. In contrast to a structure on conventionally designed foundation, which may sustain severe structural damage but can be repaired using conventional rehabilitation-strengthening techniques, the settlement and rotation of a rocking-isolated structure (even if within tolerable limits) cannot be easily repaired. Hence, even if the engineering community was convinced of the potential advantages of such design philosophy, there would still be an inherent "fear" that the deformed system would not be capable of sustaining a consecutive seismic event: a new earthquake or a strong aftershock. At least in the latter case, conventionally designed structures are also quite vulnerable. In several cases, structures that were "weakened" during a strong seismic episode, sustained severe damage (or collapsed) in an aftershock. The 2010 M_w 7.1 Darfield earthquake [Cubrinovski *et al.*, 2010] that shook the area of Canterbury in New Zealand, which was followed by two successive earthquakes (or very strong "aftershocks") during a period of 9 months (February 2011: Christchurch, M_w 6.3 ; June 2011: 10 km east of Christchurch, M_w 6.0) is perhaps one of the best examples. Even worse, in many cases damaged structures are not seriously rehabilitated (receiving only "cosmetic" repair), being hence dramatically vulnerable to future earthquakes (e.g. Meli *et al.*, 1998).

In an attempt to shed light in the resistance of the rocking-isolated system to damage accumulation due to successive earthquakes, its performance is further investigated with emphasis on the preceding shaking history. The devastating Takatori record (Kobe, 1995) is utilized as an illustrative example. Making use of the three shaking sequences (Table 2), three scenarios are considered.

(a) The seismic excitation is imposed on a newly built, undisturbed, soil-foundation-structure model (i.e., on a "virgin state," where no other shaking has taken place). *Sequence 3*, in which Takatori is the first shaking event, is utilized for this scenario.

(b) The seismic excitation is imposed on a *non-symmetrically* "weakened" model, having already sustained several real records of increasing severity. *Sequence 2*, in which Takatori is preceded by all other real records (Aegion, Lefkada, Gilroy, and Rinaldi), is utilized for this scenario.
(c) The seismic excitation is imposed on a *symmetrically* "weakened" model, having already sustained a sequence of symmetric multi-cycle artificial (sinusoidal) excitations. *Sequence 1*, in which Takatori is preceded by six sinusoidal motions of increasing severity, is utilized for this scenario.

The performance of the rocking-isolated system subjected to the three scenarios is summarized in Figs. 18 and 19, in terms of M–θ and w–θ response, and time histories of deck drift.

In all three shaking scenarios, the rocking-isolated system manages to survive the devastating Takatori record. The M–θ loops of Fig 18 reveal strongly inelastic foundation response, accompanied by substantial accumulation of settlement. The latter reaches 28 cm under "virgin state" conditions – *Scenario 1* (Fig 18a). Quite interestingly, when the

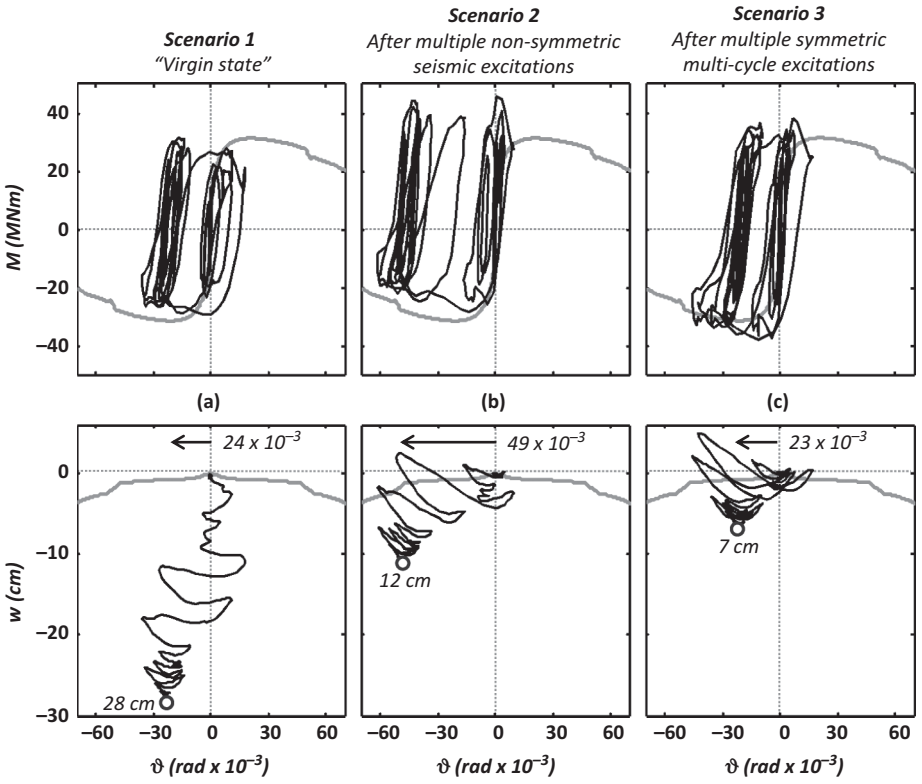

FIGURE 18 Effect of excitation history on foundation performance. Moment−rotation ($M-\theta$) and settlement– rotation ($w-\theta$) response for the rocking isolated pier during shaking with the Takatori (Kobe, 1995) record: (a) "*virgin state*" (i.e., the seismic excitation is applied to an undisturbed model); (b) after multiple non-symmetric seismic excitations (real records, characterized by directivity effects); and (c) after multiple symmetric multi-cycle (sinusoidal) excitations. The dynamic performance (black lines) is compared to the horizontal pushover response (grey lines) on undisturbed soil.

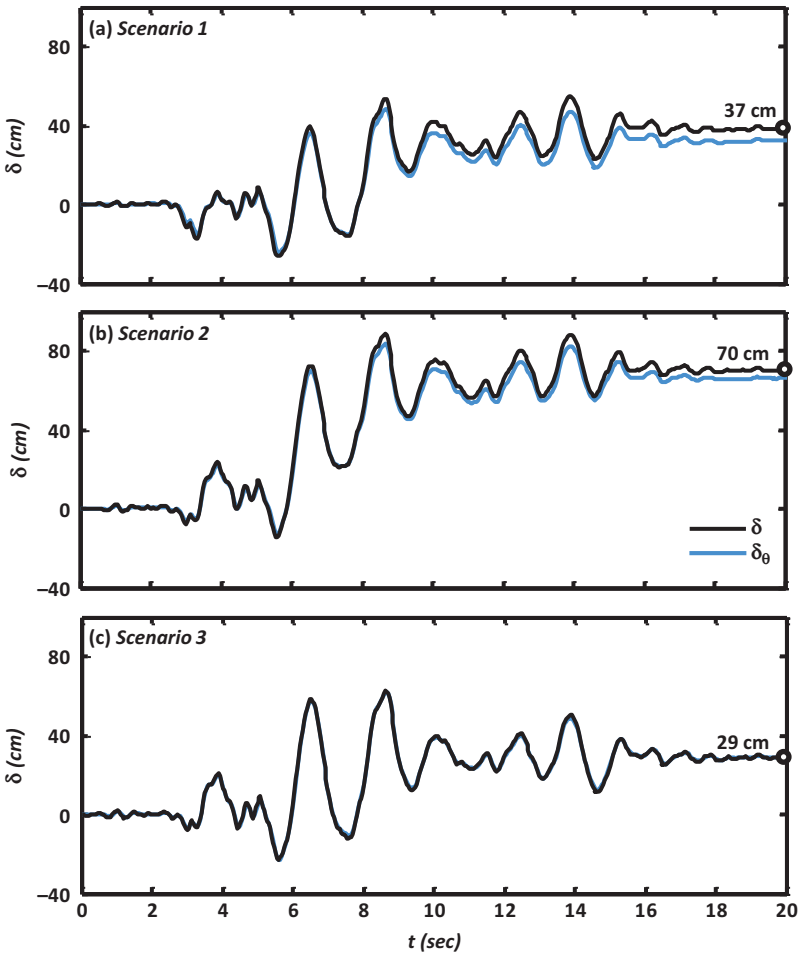

FIGURE 19 Effect of excitation history on foundation performance. Time histories of the total deck drift and its rotation induced component (δ and δ_θ, respectively) for the rocking isolated pier during shaking with the Takatori (Kobe, 1995) record: (a) "*virgin state*" (i.e., the seismic excitation is applied to an undisturbed model); (b) after multiple non-symmetric seismic excitations (real records, characterized by directivity effects); and (c) after multiple symmetric multi-cycle (sinusoidal) excitations (color figure available online).

rocking-isolated system has already sustained a number of previous shaking events, it tends to accumulate profoundly reduced settlement: 12 cm when preceded by non symmetric real records – *Scenario 2* (Fig. 18b); merely 7 cm when preceded by symmetric multi-cycle sinusoidal motions – *Scenario 3* (Fig. 18c). Such performance amelioration is presumably due to soil densification taking place during the preceding shaking events. The densification is obviously more intense in *Scenario* 3, in which the model has been subjected to 6 x $12 = 72$ strong motion cycles of increasing amplitude. As the sand becomes denser, the behavior of the foundation becomes more-and-more uplifting-dominated, as opposed to its sinking-dominated "virgin-state" response.

The differences between the three shaking history scenarios are equally pronounced when considering permanent rotation. Characterized by forward-rupture directivity effects,

the inherently asymmetric Takatori record unavoidably leads to accumulation of rotation in all three cases. The residual rotation reaches -24 x 10^{-3} rad under "virgin state" conditions — *Scenario 1* (Fig. 18a), being amplified by a factor of 2 (reaching -49 x 10^{-3} rad) when the rocking-isolated system has previously sustained non-symmetric shaking events — *Scenario 2* (Fig. 18b). In stark contrast, when the preceding seismic events are symmetric (*Scenario 3*), the accumulated permanent rotation remains practically the same (Fig 18c). This pronounced difference is directly related to the "details" of the shaking history. While in *Scenario 3*, the preceding symmetric (sinusoidal) shaking events strictly produced settlement without permanent rotation, the shaking history of *Scenario 2* includes non symmetric seismic motions (real records), which tend to accumulate settlement *and* rotation. More specifically, being also characterized by directivity effects, the Rinaldi record which precedes Takatori in *Scenario 2* led to accumulation of a non negligible rotation of -12 x 10^{-3} rad (Fig. 15b). Hence, when the already tilted system is subsequently subjected to the Takatori record, P–δ effects "facilitate" accumulation of rotation in the direction of initial tilting, leading to increased permanent rotation.

The above conclusions are clearly manifested by the time histories of deck drift (Fig. 19). In the reference case of "virgin state" conditions (*Scenario 1*) the residual drift reaches 37 cm (Fig. 19a), dramatically increasing to 70 cm when the system has already sustained non symmetric shaking events — *Scenario 2* (Fig. 19b). On the contrary, the performance is ameliorated substantially when the preceding shaking events are symmetric (*Scenario 3*): the residual deck drift is reduced to 29 cm (Fig. 19c). Observe that the differences in terms of rotational drift component δ_θ are practically negligible, which implies that the improved performance is mainly due to a reduction of the swaying component $u \approx \delta - \delta_\theta$ (for the practically rigid pier of the experiments). In addition to the previously discussed beneficial role of soil densification, this improvement is also related to embedment effects: due to the multitude of preceding multi-cycle shaking events, the foundation had become partially embedded by the time of the Takatori excitation.

It should be emphasized that the presented example corresponds to an extreme shaking scenario, utilized herein to illustrate the resistance against cumulative damage of the rocking-isolated system, which survives toppling collapse even when subjected to such an improbable sequence of seismic events. Nevertheless, even by the end of such unrealistically harsh shaking sequences (in which the pier has been previously subjected to six symmetric multi-cycle motions, or to four non-symmetric shaking events with at least one of them, Rinaldi, being particularly detrimental), the rocking-isolated system appears to be stable without an evident risk of incipient toppling collapse.

7. Summary and Conclusions

Aiming to verify the seismic performance of rocking-isolated structures, and to provide experimental evidence supporting the findings of analytical studies, this article experimentally investigated the seismic performance of an idealized bridge pier supported on a surface foundation. A series of reduced-scale shaking table tests were conducted, considering two design alternatives: (a) conventionally over-designed foundation; and (b) rocking isolation, in which the foundation is deliberately under-designed to promote uplifting, acting as seismic isolation and guiding plastic deformation to the soil-foundation interface. The two design alternatives were subjected to a variety of shaking events, comprising real records and artificial sinusoidal motions of varying intensity. Three different shaking sequences were performed in order to shed light in the performance of rocking-isolated structures subjected to successive seismic events.

The main conclusions of the present study can be summarized as follows.

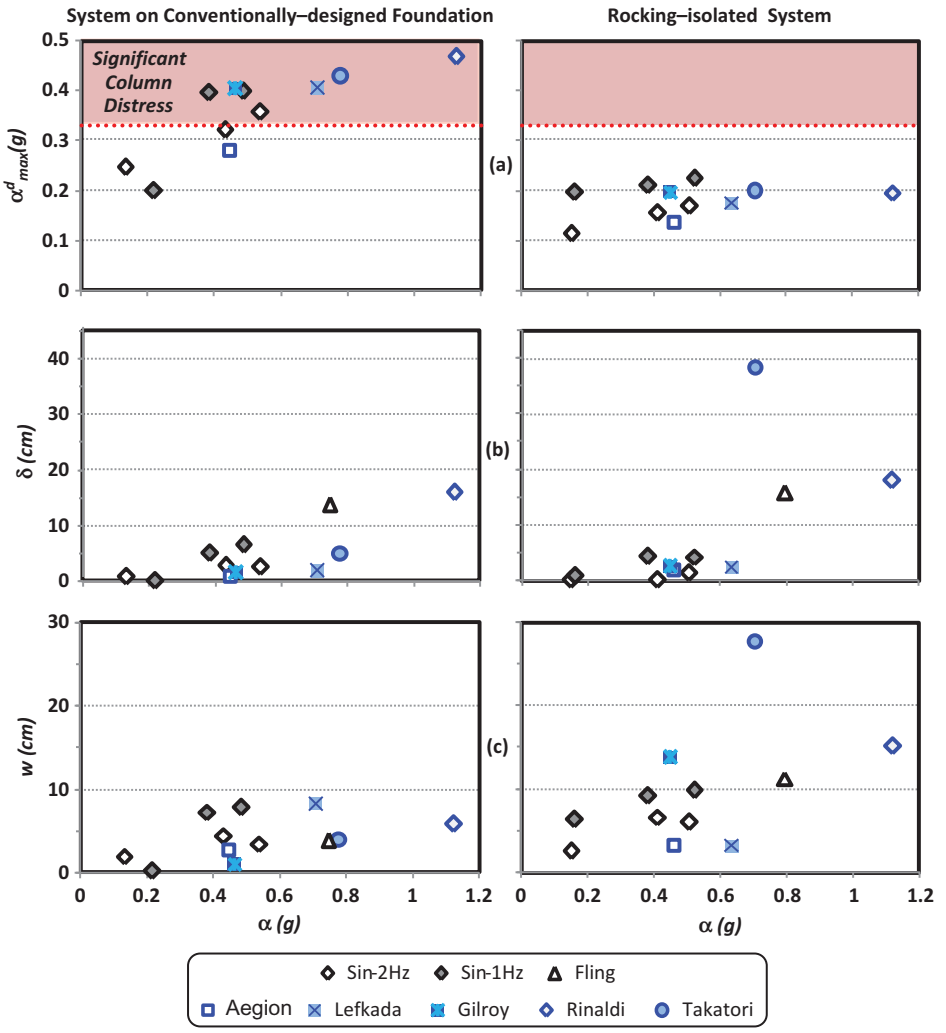

FIGURE 20 Synopsis of shaking table test results. Comparative performance assessment of the two design alternatives in terms of: (a) maximum deck acceleration; (b) maximum deck drift; and (c) foundation settlement with respect to the maximum acceleration of the seismic excitation (color figure available online).

1) As summarized in Fig. 20, rocking isolation is proven quite effective in reducing the inertia forces transmitted onto the superstructure. The deck acceleration cannot exceed $\alpha_c \approx 0.2$ g, being constrained by the moment capacity of the under-designed foundation (Fig. 20a). Hence, the RC pier is effectively protected, surviving all seismic excitations without structural damage. In stark contrast, the system on conventionally designed foundation would tend to develop inertia forces in excess of the capacity of the RC pier: having $M_u{}^P \approx 46$ MNm, the pier can sustain $\alpha_{max} \approx 0.32$ g. Hence, with the exception of moderate intensity seismic events (such as Aegion), a certain degree of structural damage would be unavoidable. Although the inelastic response of the pier was not modeled in the experiments — a limitation of the present study, the degree of structural damage can be qualitatively assessed on

the basis of the ratio of ductility demand to ductility capacity (which is a function of the recorded deck acceleration and of the α_{max} that the pier can sustain).

2) The aforementioned acceleration cutoff is accompanied by an increase of maximum and residual deck drift (Fig. 20b), and of permanent settlement (Fig. 20c). In terms of deck drift, with the exception of the devastating Takatori record, the differences between the two design alternatives are not as pronounced. In reality, however, the system on conventionally designed foundation would be subjected to pier bending failure, unavoidably experiencing additional drift due to plastic flexural distortion. Hence, if the inelastic response of the RC pier had been accounted for, the comparison would possibly be even more in favor of the rocking-isolated alternative. Consequently, the increase of permanent settlement seems to be the only substantial drawback of rocking-isolation.
3) An additional potential drawback of rocking isolation is related to the "fear" that such systems may be sensitive to rapid strength degradation when subjected to multiple cycles of loading. The validity of this argument was investigated by comparing the performance of the *rocking-isolated* system with that of a well-confined RC pier from the literature [Lehman and Moehle, 1998]. It is concluded that the performance of the rocking-isolated system is advantageous, having substantially larger margins of safety against collapse. Being remarkably resistant to cumulative cyclic loading, when subjected to a cyclic drift ratio δ/h of the order of 5.5%, the rocking-isolated system exhibits limited strength degradation not exceeding 25%. At the same δ/h level, the conventional system is just about to collapse, experiencing abrupt strength degradation in excess of 50%. In contrast to a conventionally designed system, where the loss of strength is due to damage accumulation in the "plastic hinge," in a rocking-isolated system it is mainly due to P–δ effects. Therefore, it can reasonably be argued that the rate of strength degradation will not change with further increase of δ/h.
4) Another commonly postulated potential disadvantage of rocking isolation is related to the risk of damage accumulation in successive seismic events. The validity of this argument was investigated by comparing three distinctly different shaking sequences, imposing strong seismic shaking: (a) on an undisturbed model; (b) on a non-symmetrically "weakened" model, having sustained several real records; and (c) on a symmetrically "weakened" model, having sustained a sequence of symmetric multi-cycle sinusoidal excitations. The following is concluded.

- When the rocking-isolated system has sustained a number of shaking events (symmetric or not), it tends to accumulate substantially reduced settlement. Such performance amelioration is presumably due to soil densification taking place during the preceding shaking events.
- With respect to rotation, the performance is more sensitive to the "details" of the shaking history. When the preceding seismic events are symmetric, the rotational response is practically insensitive to the shaking history. In stark contrast, when the preceding seismic events are non symmetric (such as the directivity-affected records of this study), the system accumulates settlement *and* rotation. Consequently, when the already tilted system is subjected to the next seismic event, it is prone to increased accumulation of rotation.
- Nevertheless, the rocking-isolated system of this study survives toppling collapse even when subjected to a highly improbable sequence of seismic events. By the end of such unrealistically harsh shaking sequence (in which the model has already sustained six symmetric, or four non symmetric shaking events),

the rocking-isolated system remains stable without an evident risk of incipient toppling collapse.

Acknowledgment

The financial support for this article was provided under the research project "DARE," which is funded through the European Research Council's (ERC) "IDEAS" Programme, in Support of Frontier Research–Advanced Grant, under contract/number ERC–2–9–AdG228254–DARE to Professor G. Gazetas.

Notation List

A_E	Maximum acceleration at bedrock
B	In-plane foundation breadth
d_{10}	Maximum grain size of the finest 10%
d_{50}	Mean grain size
d_{60}	Maximum grain size of the finest 60%
D_r	Relative density
e_{max}	Void ratio at loosest state
e_{min}	Void ratio at densest state
FS	Factor of safety
FS_E	Factor of safety in combined N−Q−M loading
FS_V	Factor of safety in pure vertical loading
h	Height of the oscillator
h_f	Foundation height
h_p	Distance from the top of the foundation to the center of mass
$K^{SSI,lin}$	Linear-elastic stiffness taking account of SSI
$K^{SSI,nl}$	Secant stiffness taking account of nonlinear SSI
L	Out-of-plane foundation breadth
M	Moment load
m	Mass
M_{ult}	Ultimate moment load
N	Vertical load
n	Modeling scale
N_{ult}	Ultimate vertical load
Q	Shear load
q	Behavior factor
S_a	Spectral acceleration
T	Period
T^0	Fixed base period
$T^{SSI,lin}$	Linear-elastic response period taking account of SSI
$T^{SSI,nl}$	Response period taking account of nonlinear SSI
u	Foundation horizontal translation (swaying component)
w	Foundation settlement
α	Acceleration at the center of mass
α_c	Critical acceleration ($a_c = M_{ult}/mgh$)
α_{max}	Maximum acceleration at the center of mass
δ	Deck total drift
δ_θ	Deck drift due to foundation rotation

θ	Foundation rotation
ξ	Damping ratio
ϕ	Soil friction angle
P	Lateral load at the deck
P_{ult}	Ultimate lateral load at the deck
μ^{Δ}	Displacement ductility
A_g	Column gross cross section area
f_c	Concrete compression strength
${\alpha_c}^{max}$	Maximum acceleration developed at the deck

References

Algie, T. B., Deng, L., and Kutter, B. L. [2009] "Centrifuge tests of rocking shallow bridge foundations," *Proc. of the 2009 NZSEE Conference*, Christchurch, New Zealand, pp. 6–8.

Allotey, N. and El Naggar, M. H. [2008] "An investigation into the Winkler modelling of the cyclic response of rigid footings," *Soil Dynamics & Earthquake Engineering* **28**(1), 44–57.

Anastasopoulos, I., Gazetas, G., Loli, M., Apostolou, M., and Gerolymos, N. [2010a] "Soil failure can be used for seismic protection of structures," *Bulletin of Earthquake Engineering* **8**(2), 309–326.

Anastastasopoulos, I., Georgarakos, P., Georgiannou, V., Drosos, V., and Kourkoulis, R. [2010b] "Seismic performance of bar-mat reinforced-soil retaining wall: shaking table testing versus numerical analysis with modified kinematic hardening constitutive model," *Soil Dynamics & Earthquake Engineering* **30**, 1089–1105.

Anastasopoulos, I., Gelagoti, F., Kourkoulis, R., and Gazetas, G. [2011] "Simplified constitutive model for simulation of cyclic response of shallow foundations: validation against laboratory tests," *Journal of Geotechnical and Geoenvironmental Engineering* ASCE **137**(12), 1154–1168.

Apostolou, M., Gazetas, G., and Garini, E. [2007] "Seismic response of slender rigid structures with foundation uplifting," *Soil Dynamics and Earthquake Engineering* **27**(7), 642–654.

Applied Technology Council [1996] "The seismic evaluation and retrofit of concrete buildings," *Report ATC 40*, Redwood City, CA.

Beck, J. and Skinner, R. I. [1974] "The seismic response of a reinforced concrete bridge pier designed to step," *Earthquake Engineering & Structural Dynamics* **2**(4), 637–655.

Butterfield, R. and Gottardi, G. [1994] "A complete three dimensional failure envelope for shallow footings on sand," *Géotechnique* **44**(1), 181–184.

Chai, Y. H., Priestley, M. J. N., and Seible, F. [1991] "Seismic retrofit of circular bridge columns for enhanced flexural performance," *ACI Structural Journal* **88**(5), 572–585.

Chatzigogos, C. T., Pecker, A., and Salencon, J. [2009] "Macroelement modelling of shallow foundations," *Soil Dynamics & Earthquake Engineering* **29**, 765–781.

Chen, Y. H., Liao, W. H., Lee, C. L., and Wang, Y. P. [2006] "Seismic isolation of viaduct piers by means of a rocking mechanism," *Earthquake Engineering & Structural Dynamics* **35**(6), 713–736.

Crémer, C., Pecker, A., and Davenne, L. [2001] "Cyclic macro-element for soil–structure interaction: material and geometrical nonlinearities," *International Journal for Numerical and Analytical methods in Geomechanics* **25**(12), 1257–1284.

Cubrinovski, M., Green, R., Allen, J., Ashford, S., Bowman, E., Bradley, B. A., Cox, B., Hutchinson, T., Kavazanjian, E., Orense, R., Pender, M., and Wotherspoon, L. [2010] *Geotechnical Reconnaissance of the 2010 Darfield (New Zealand) Earthquake, Report*, University of Canterbury, Christchurch, New Zealand.

Dowdell, D. J. and Hamersley, B. A. [2000] "Lions' Gate Bridge North Approach — Seismic retrofit," in *Behaviour of Steel Structures in Seismic Areas*, *Proc. of STESSA*, Montreal, Canada, pp. 319–326.

Drosos, V., Georgarakos, T., Loli, M., Anastasopoulos, I., Zarzouras, O., and Gazetas, G. [2012] "Soil–foundation–structure interaction with mobilization of bearing capacity: An experimental study on sand," *Journal of Geotechnical and Geoenvironmental Engineering* ASCE **138**(11), 1–18.

EC8 [2000] *Design Provisions for Earthquake Resistance of Structures, Part 5 : Foundations, Retaining Structures and Geotechnical Aspects*, prEN, 1998-5 European Committee for Standardization, Brussels.

Faccioli, E., Paolucci, R., and Vivero, G. [2001] "Investigation of seismic soil–footing interaction by large scale cyclic tests and analytical models," *Proc. of the 4th Int. Conf. in Recent Advances in Geotechnical Earthquake Engineering and Soil Dynamics*, San Diego, pp. 26–31.

FEMA [1997] *NEHRP Guidelines of the Seismic Rehabilitation of Buildings*, Federal Emergency Management Agency, Publication No. 356, Washington, D.C.

Figini, R., Paolucci, R., and Chatzigogos, C. T. [2012] "A macro-element model for non-linear soil–shallow foundation–structure interaction under seismic loads: theoretical development and experimental validation on large scale tests," *Earthquake Engineering & Structural Dynamics* **41**(3), 475–493.

Gajan, S., Kutter, B., Phalen, J., Hutchinson, T., and Martin, G. [2005] "Centrifuge modeling of load-deformation behavior of rocking shallow foundations," *Soil Dynamics and Earthquake Engineering* **25**, 773–783.

Gajan, S. and Kutter, B. [2008] "Capacity, settlement, and energy dissipation of shallow footings subjected to rocking," *Journal of Geotechnical and Geoenvironmental Engineering ASCE* **135**(3), 407–420.

Gajan, S. and Kutter, B. [2009] "Contact interface model for shallow foundations subjected to combined loading," *Journal of Geotechnical and Geoenvironmental Engineering ASCE* **134**(8), 1129–1141.

Gelagoti, F., Kourkoulis, R., Anastasopoulos, I., and Gazetas, G. [2012] "Rocking isolation of frame structures founded on separate footings," *Earthquake Engineering & Structural Dynamics* **41**, 1177–1197.

Gourvenec, S. [2007] "Shape effects on the capacity of rectangular footings under general loading," *Géotechnique* **57**(8), 637–646.

Grange, S., Kotronis, P., and Mazars, J. [2008] "A macro-element for the circular foundation to simulate 3D soil-structure interaction," *International Journal for Numerical and Analytical Methods in Geomechanics* **32**, 1205–1227.

Houlsby, G. T., Amorosi, A., and Rojas, E. [2005] "Elastic moduli of soils dependent on pressure: a hyperelastic formulation," *Géotechnique* **55**(5), 383–392.

Housner, G. W. [1963] "The behavior of inverted pendulum structures during earthquakes," *Bulletin of the Seismological Society of America* **53**(2), 404–417.

Huckelbridge, A. A. and Ferencz, R. M. [1981] "Overturning effects on stiffened building frames," *Earthquake Engineering & Structural Dynamics* **9**(1), 69–83.

Hung, H., Liu, K., Ho, T., and Chang, K. [2011] "An experimental study on the rocking response of bridge piers with spread footing foundations," *Earthquake Engineering & Structural Dynamics* **40**(7), 749–769.

Kourkoulis, R., Gelagoti, F., Anastasopoulos, I. [2012] "Rocking isolation of frames on isolated footings: design insights and limitations," *Journal of Earthquake Engineering* **16**(3), 374–400.

Kutter, B. L., Martin, G., Hutchinson, T. C., Harden, C., Gajan, S., and Phalen, J. D. [2003] "Status report on study of modeling of nonlinear cyclic load–deformation behavior of shallow foundations," PEER Workshop, University of California, Davis, California.

Lehman, D. E. and Moehle, J. P. [1998] "Seismic performance of well-confined concrete bridge columns," *PEER report 1998/01. 2000*, University of California Berkley.

Meek, J. W. [1975] "Effect of foundation tipping on dynamic response," *Journal of the Structural Division ASCE* **101**(7), 1297–1311.

Meli, R., Faccioli, E., Murià-Vila, D., Quaas, R., and Paolucci, R. [1998] "Study of site effects and seismic response of an instrumented building in Mexico City" *Journal of Earthquake Engineering* **2**, 89–111.

Mergos, P. E. and Kawashima, K. [2005] "Rocking isolation of a typical bridge pier on spread foundation," *Journal of Earthquake Engineering* **9**(2), 395–414.

Meyerhof, G. G. [1951] "The ultimate bearing capacity of foundations," *Géotechnique* **2**(4), 301–332.

Muir Wood, D. [2004] *Geotechnical Modelling*, Spon Press, London.

Negro, P., Paolucci, R., Pedretti, S., and Faccioli, E. [2000] "Large-scale soil–structure interaction experiments on sand under cyclic loading," *Proc. of the 12th World Conference on Earthquake Engineering*, Auckland, New Zealand, Paper 1191.

Palmeri, A. and Makris, N. [2008] "Response analysis of rigid structures rocking on viscoelastic foundation," *Earthquake Engineering & Structural Dynamics* **37**(7), 1039–1063.

Panagiotidou, A. I., Gazetas, G., and Gerolymos, N. [2012] "Pushover and seismic response of foundations on stiff clay: Analysis with P-Δ effects," *Earthquake Spectra* **28**(4), 1–30.

Paolucci, R. [1997] "Simplified evaluation of earthquake induced permanent displacements of shallow foundations," *Journal of Earthquake Engineering* **1**(3), 563–579.

Paolucci, R., Shirato, M., and Yilmaz, M. T. [2008] "Seismic behaviour of shallow foundations: Shaking table experiments *vs* numerical modeling," *Earthquake Engineering and Structural Dynamics* **37**, 577–595.

Pecker, A. [2005] "Design and construction of the foundations of the Rion Antirion Bridge," *Proc. of the 1st Greece–Japan Workshop on Seismic Design, Observation, Retrofit of Foundations*, Athens, pp. 119–130.

Priestley, M. J. N. and Seible, F. [1995] "Design of seismic retrofit measures for concrete and masonry structures," *Construction and Building Materials* **9**(6), 365–377.

Priestley, M. J. N., Seible, F., and Calvi, G. M. [1996] *Seismic Design and Retrofit of Bridges*, John Wiley & Sons, New York.

Raychowdhury, P. and Hutchinson, T. C. [2009] "Performance evaluation of a nonlinear Winkler-based shallow foundation model using centrifuge tests results," *Earthquake Engineering & Structural Dynamics* **38**(5), 679–698.

Sakellaraki, D. and Kawashima, K. [2006] "Effectiveness of seismic rocking isolation of bridges based on shake table tests," *Proc. of the 1st European Conference on Earthquake Engineering and Seismology*, Geneva, Switzerland, pp. 1–10.

Seible, F., Priestley, M. J. N., and MacRae, G. [1995] "The Kobe earthquake of January 17, 1995; initial impressions from a quick reconnaissance," *Structural Systems Research Report-95/03*, University of California, San Diego..

Sezen, H. [2002] "Seismic behavior and modeling of reinforced concrete building columns", Ph.D. dissertation, Dept. of Civil and Environmental Engineering, University of California, Berkeley.

Shirato, M., Kouno, T., Asai, R., Nakani, N., Fukui, J., and Paolucci, R. [2008] "Large-scale experiments on nonlinear behaviour of shallow foundations subjected to strong earthquakes," *Soils & Foundations* **48**(5), 673–692.

Taiebat, H. A. and Carter, J. P. [2000] "Numerical studies of the bearing capacity of shallow foundations on cohesive soil subjected to combined loading," *Geotechnique* **50**(4), 409–418.

Yashinsky, M. and Karshenas, M. J. [2003] *Fundamentals of Seismic Protection for Bridges*, EERI Monograph MNO-9, Oakland, CA.

Yim, S. C. and Chopra, A. K. [1985] "Simplified earthquake analysis of structures with foundation uplift," *Journal of Structural Engineering*, *ASCE* **111**(4), 906–930.

Zhang, J. and Makris, N. [2001] "Rocking response of free-standing blocks under cycloidal pulses," *Journal of Engineering Mechanics* **127**(5), 473–483.